MICROCOPY RESOLUTION TEST CHART

NATIONAL BUREAU OF STANDARDS-1963-A

AD A138057
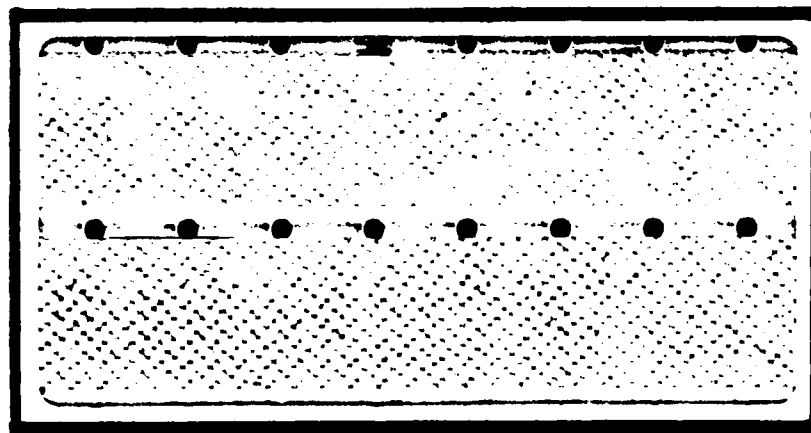
DTIC
ELECTE
FEB 2 2 1984
S

DEPARTMENT OF THE AIR FORCE

AIR UNIVERSITY

AIR FORCE INSTITUTE OF TECHNOLOGY

Wright-Patterson Air Force Base, Ohio

84 02 21 172

MICROWAVE EXCITATION

OF A CO_2 LASER

THESIS

AFIT/GEP/PH/83D-8   Richard C. Page

Capt   USAF

FEB 2 2 1984

MICROWAVE EXCITATION

OF A CO_2 LASER

THESIS

Presented to the Faculty of the School of Engineering

of the Air Force Institute of Technology

Air University

In Partial Fulfillment of the

Requirements for the Degree of

Master of Science

by

Richard C. Page

Capt   USAF

Graduate Engineering Physics

December 1983

Preface

This topic was among the last topics presented to the GEP 83-D class as a possible thesis project. The subject seemed to be complex but exciting. I was correct on both points.

I wish to clarify the units I used in this report. I have always found the rationalized MKS units the easiest to use. All equations referenced in the text are in MKS units, unless noted otherwise. Distances are measured in centimeters, which is consistent with most of the literature in this area of study. While not strictly MKS units, centimeters, as with other distances, are a simple transformation to convert to the MKS system of units. Equations involving electric and magnetic fields in CGS-ESU units, on the other hand, do not transform as directly to MKS units.

I express my gratitude to Dr. Alan Garscadden for suggesting this topic and his helpful suggestions and guidance throughout the project. I thank Dr. Merrill Andrews who helped me in all phases of the experimental effort.

Special thanks go to my thesis advisor, Dr. William Bailey, who was always willing to discuss the significance of observations made, often on little or no notice. His ability to make back of the envelope calculations and

estimations of expected results have given me a great respect of the value and power of making intelligent estimates of parameters.

Considerable equipment had to be built and some existing equipment had to be modified for this research effort. Mr. Bob Knight did much of this work, delivering exactly what was wanted. Mr. Jimmy Ray did all glass work for this project. He often went out of his way to help when I needed glassware support. My thanks also go to the many people who allowed me to borrow various pieces of equipment. Their unselfish cooperation in scheduling their own work so I had access to some of the equipment, made much of this effort possible.

Most of all, I thank my wife, Cindy; and daughter, Jeanine, for their loving support while I was working on this project.

Contents

List of Figures

Notation

c   - Speed of light $\cong$ 3.00×10^8 m/s

cm - Centimeter

d   - Distance between electrodes (cm)

e   - Elementary charge $\cong$ 1.60×10^{-19} coul

eV - Electron volts

f_p - Plasma frequency (Hz)

h   - Planck's constant $\cong$ 6.63×10^{-34} joule-sec

id - Inside diameter

k   - Boltzmann's constant $\cong$ 1.38×10^{-23} joule/$^\circ$K

kV - Kilovolts

kW - Kilowatts

m   - Mass (kg)

m   - Meter

m_e - Rest mass of elctron $\cong$ 9.11×10^{-31} kg

ma - Milliamperes

mw - Milliwatts

n   - Neutral particle density (cm^{-3})

n_0 - Initial electron density (cm^{-3})

n_e - Electron density (cm^{-3})

n_N^* - Density of vibrationally excited N_2 (cm^{-3})

p   - Pressure (torr)

$q_{1,2}$ - Gaussian beam parameter

r   - Radius of tube (cm)

s   – Momentum collision cross section (cm^2)

t   – Time (sec)

usec– Microsecond (10^{-6} sec)

v_{de} – Drift velocity of electrons (cm/sec)

v_{di} – Drift velocity of ions (cm/sec)

v_e – Electron thermal velocity (cm/sec)

v_i – Ion thermal velocity (cm/sec)

x   – Distance (cm)

z_0 – Location of waist of gaussian beam (cm)

B   – Magnetic field (nt/amp-m)

D   – Diameter of mirror (cm)

D   – Diameter of discharge tube (cm)

D_a – Ambipolar diffusion coefficient (cm^2/sec)

D_i – Ion diffusion coefficient (cm/sec)

E   – Electric field (volt/cm)

E_0 – Electric field (volt/cm)

E_{eff}– Effective electric field (volt/cm)

G   – Gain

$G_{1,2}$– Dimensionless parameter used in Gaussian beam calculations

GHz – Gigahertz (1×10^9 sec^{-1})

Hz   – Hertz (sec^{-1})

I   – Current (amp)

J   – Current density (amp/cm^2

L   – Resonator cavity length (cm)

L_{atc}– Attachment loss rate of electrons (sec^{-1}/cm^3)

L_{dif}– Diffusion loss rate of electrons (sec^{-1}/cm^3)

MHz – Megahertz (1×10^6 sec^{-1})

P_{ion}– Power used in ionization of gas (watts)

R – Universal gas constant $\equiv$ 8.31 joule/^{O}K

R – Radius of curvature of wave front (m)

R_b – Resistance of ballast resistor (ohms)

R_l – Recombination loss coefficient (cm^3/sec)

$R_{1,2}$– Radius of curvature of cavity mirrors (m)

SCCM– Standard cubic centimeters per second (cm^3/sec)

S_{ext}– External source rate of electrons (sec^{-1}/cm^3)

T – Temperature (^{O}K, eV)

T_e – Electron temperature (eV, ^{O}K)

V – Applied potential (volts)

V_a – Characteristic arc potential (volt)

V_g – Glow discharge minimum potential (volt)

V_{min}– Minimum static breakdown potential (volt)

V_s – Static breakdown potential (volt)

V_{sup}– Supply potential (volt)

W_0 – Gaussian beam waist size

Y – Wavelength (cm)

Λ – Characteristic length for diffusion (cm)

ϵ_0 – Permitivity of free space $\equiv$ 8.85x10^{-12} farad/m

π – $\equiv$ 3.14159

σ – Momentum collision cross section (cm^2)

τ_e – Electron lifetime (sec)

μ_0 – Permeability of free space $\equiv$1.26x10^{-6} henry/m

ν_c – Collision frequency per electron (sec^{-1})

ν_f - Collision frequency per ion (sec^{-1})

ν_i - Ionization rate per electron (sec^{-1})

ω - Frequency (rad/sec)

ω_p - Plasma frequency (rad/sec)

λ_D - Debye length $\equiv$ 740 kT/n$_e$ (eV^{-1}-cm^{-2})

λ_s - Skin depth

ABSTRACT

A flowing carbon dioxide laser was operated at low pressures up to 4 torr. Excitation of the laser was provided using various combinations of direct current (DC), pulsed microwave, and continuous wave (CW) microwave excitation. The microwaves were in the 2.45 GHz band and were coupled into the gas using a slow-wave interdigital transmission line. Laser output of 25 milliwatts (mw) was achieved using a DC discharge only. A combination of a DC discharge and pulsed microwaves doubled the output and resulted in some modulation. Changing the laser gas mixture and pulsed microwave field characteristics allowed some flexibility in the modulation. Lasing was not achieved with excitation from the CW microwaves alone due to the formation of localized discharges. Using pulsed microwaves to sustain the discharge and CW microwaves to pump the laser, a quasi-CW output of 55 mw was achieved.

I. Introduction

Spectroscopic analysis of materials often requires the use of tunable light sources in the wavelength region of interest. Lasers are a valuable tool which enable this to be done, providing both the desired narrow bandwidth and intensities higher than is possible with other light sources.

The main thrust of the work presented here is to experimentally investigate an electrodeless laser using microwaves as the sole pumping source. A desired result of this research is to make it possible to build an electrodeless laser which would be easy to construct in the laboratory environment and provide some degree of portability.

Electrodeless discharges offer distinct advantages. Gases which would normally react with common electrode materials could be used without having to develop an electrode material for each gas. Sealed-off operation would be facilitated when laser gas contamination from the electrodes is eliminated. Tube construction would be simplified. The frequency range could be selected by inserting a tube containing the desired laser gas mixture.

The method to be investigated is the pumping of a

1

laser with microwaves. This research will be limited to a CO_2 laser because of the relative ease this gas can be made to lase. While no other types of lasers will be considered in this work, many of the same techniques and principles should apply to other molecular gas laser systems.

Lasers pumped by microwaves have immediate applications in the military environment. Existing radar systems could use microwave-pumped lasers for jam-resistant and low probability of enemy detection air-air communication.

Background

Lasing of pure CO_2 in the infrared region was first reported in 1964 by Patel. Advances were rapidly made so that power had been increased from the original 1 mw by Patel et al to 8.8 kW by Horrigan et al in 1969. Efficiencies were increased from 10^{-6} to 0.05 during a period of about one year since the invention of the CO_2 laser [Ref 9:1-2].

Many CO_2 lasers rely on a flow of fresh laser gases in operation. Flowing gas through the laser purges contaminants which result from processes such as dissociation of the gases, reaction of the dissociated gases with the electrodes and outgassing of the electrodes. Progress has been made in sealed off operation of CO_2 lasers with lifetimes in the thousands of hours reported. Some schemes require interrupted operation to rejuvenate

2

the tube by heating the electrodes to reverse chemical reactions caused by dissociation [Ref 9:19-20].

Work has been done with CO_2 lasers using radio frequency (rf) methods for transverse excitation [Ref 15:652-653; 19:13-15] but is usually limited to waveguide lasers because of the dimensions involved.

Handy & Brandelik showed that a CO_2 laser could be pumped with pulsed 2.45 GHz microwave radiation [Ref 11]. Similar work was done by Vasyutinskii, et al [Ref 25] at 2.7 GHz. In the work by Handy & Brandelik, the laser plasma tube was inserted in a waveguide which was tapered to increase the electric field strength. The tube axis was perpendicular to the direction of microwave propagation. In the research by Vasyutinskii, the plasma tube was inserted in a standard waveguide with the tube axis parallel to the direction of microwave propagation.

Problem

Establish lasing in a CO_2:N_2:He gas mixture using 2.45 GHz microwave radiation to pump the laser medium.

Assumptions

The pressure difference between the plasma tube and pressure detectors due to gas viscosity is assumed to be negligible for the results presented here. Gas pressure changes were made during the course of the experiments with little or no change in observed laser output values.

The meters for the crystal detectors are assumed to be

calibrated for CW microwaves since the exact field strength at the applicator is not known [Ref 6]. The crystals were calibrated in 1982.

Power output of the pulsed sources is assumed to be 30% of the power input to the microwave tube. This assumption is made because the detection crystals are not calibrated for the pulsed microwaves.

IIa. DC Discharges

This section covers the three basic types of direct current (DC) discharges and reviews some of their characteristics. Emphasis will be made on the glow discharge, which has the most direct application to this work. This section also includes concepts useful in the study of discharges and gives characteristic values for those applicable to this research.

Types of DC Discharges

DC discharges may be classified in three basic categories--Townsend, glow (normal and abnormal glow), and arc. All gases exhibit electrical breakdown when sufficient voltage is applied to a region of the gas. A quantity called the static breakdown potential (V_s) is the minimum potential at which sparking will occur in the gas.

When the applied voltage to a gas is exactly V_s, an ionization current exists. This discharge is called a Townsend discharge and is characterized by small currents.

Gases typically exhibit a negative resistance in the glow discharge. In the transition from Townsend to normal glow discharges, the potential between the electrodes decreases while the current increases [Ref Fig 1].

5
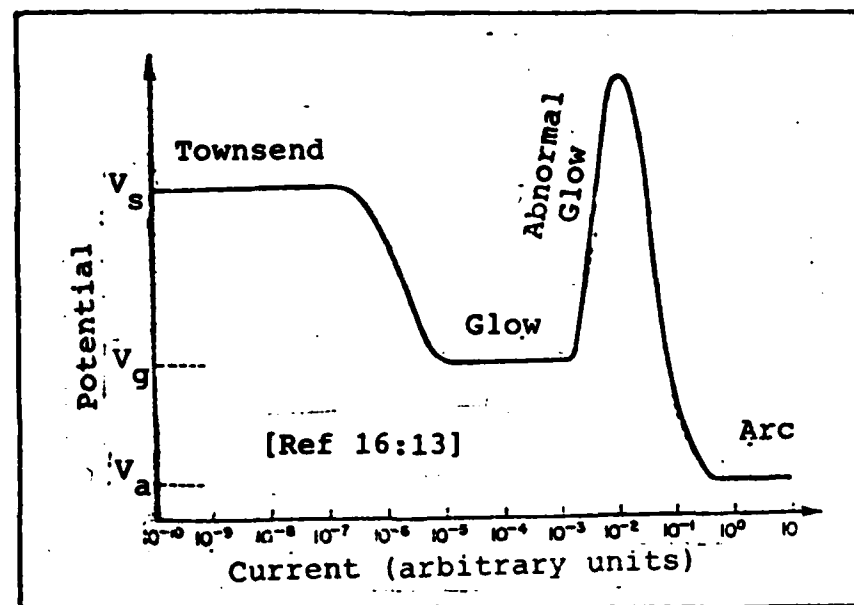
Figure 1. Self-sustained discharge characteristics.
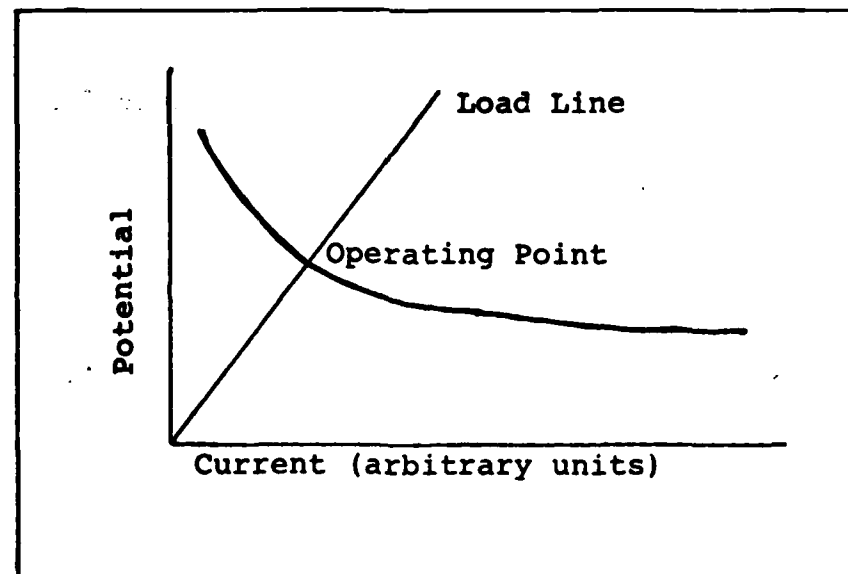
Figure 2. Characteristic I-V plot (linear) of a gas. The load line represents the resistance of the gas and establishes the operating point.

6

As current is increased in the normal glow discharge region, the potential between the electrodes remains almost constant at a characteristic value V_g. To properly limit the current and force the operating point of the gas to be within the glow discharge region, a ballast resistor of resistance R_b is placed in series with the power supply-discharge tube circuit so that

$$V_{sup} - V_g = R_b I_d \qquad (1)$$

where V_{sup} is the supply voltage, and I_d is the desired discharge current. The operating point of a gas discharge will be established by the current as a result of the current- voltage (I-V) characteristics [Ref Fig 2] for the gas in a particular geometry.

If the current is increased past the normal glow region, the abnormal glow discharge is obtained. This is characterized by an increase in potential between the electrodes and substantial increases in heating of the gas.

Any additional increase in current results in an arc, a rapid and uncontrolled discharge. The arc is characterized by high electron densities, high conductivity (high currents possible), and low electron temperatures. Tremendous gas heating (1000's of $^\circ$K) and dissociation result from increased number of collisions from the higher electron density. In an arc discharge, the cathode may be subjected to sputtering, which can result in contamination

7

of the gas and electrode erosion. The heat generated can quickly destroy a tube not designed to operate in this type of discharge.

Electron Density

The primary charge carrier in a gas discharge is the electron. If no free electrons are present, there will be no discharge. In a steady state condition, which will be the primary emphasis in this section, the density of electrons as well as the density of neutrals and ions remain constant. The conservation of electrons can now be considered. The time derivative of the electron density is

$$\frac{d\,n_e}{d\,t} = \nu_i\,n_e + S_{ext} - R_1 n_e^2 - D_a\,\nabla^2 n_e - L_{atc} \tag{2}$$

where n_e is the electron density, ν_i is the average ionization frequency per electron, S_{ext} is the external source of electrons, R_1 is the recombination loss coefficient, D_a is the ambipolar diffusion coefficient, and L_{atc} is the attachment loss rate. The electron density in the recombination term is squared because recombination is proportional to the densities of both electrons and ions. Only n_e is used because the electron density is approximately equal to the ion density.

In a steady state, the total rate of creation of electrons must equal the total rate of all loss processes. In general, recombination is insignificant at low electron

8

densities [Ref 20:33] so this term will be ignored.

The electron density can be estimated from the current flowing through the discharge using the relation

$$J = n_e e \, v_{de} \tag{3}$$

where J is the current density, e is the fundamental unit of charge, and v_{de} is the drift velocity of the electrons due to the applied field. Nominal DC current densities of 20 ma/cm^2 were used in the experiments here. Drift velocities for electrons in a 1:1:8 (CO_2:N_2:He) discharge will vary from 2×10^6 cm/sec for electric field to gas particle density ratio (E/N) of 10^{16} V-cm^2 to 2×10^7 cm/sec for an E/N ratio of 10^{15} V-cm^2 [Ref 18:28]. The resultant electron densities lie between 6×10^{10}/cm^3 to 6×10^9/cm^3. These estimates are values expected in the laser under consideration.

Collision Frequency

Electrons collide with the gas constituents in both elastic and inelastic processes. It is through these interactions that energy of the electrons are transferred to the other particles in the gas. The collision frequency of an electron with colliding partners is given by

$$\nu_c = n \, \sigma \, v_e \qquad \text{[Ref 14:75]} \tag{4}$$

where v_e is the electron velocity and σ is the average momentum collision cross section between the electron and the colliding partner. For the gases under consideration, the collision cross section is in the order of 10^{-16} cm^2. For gases at 1 torr and 400° K the particle density is 2.4×10^{16}/cm^3. Electron energies are estimated at 2 eV (8×10^7 cm/sec) for the work here. The result is collision frequencies near 2×10^8/sec can be expected for electrons.

Diffusion Loss

The mathematical form of the diffusion loss term is $d\, n_e/d\, t = -D_a \nabla^2 n_e$ where D_a is the ambipolar diffusion coefficient. The solution can be obtained by using separation of variables [Ref 4:137-144]. In cylindrical coordinates the solution for the decay of an initial distribution is

$$n_e = n_0 \exp(-t\, D_a\, 2.4^2\, /\, r^2) \tag{5}$$

[Ref 25:191]

where n_0 is the initial electron density and r is the radius of the discharge tube. In the steady state with ionization present the diffusion loss would be the same as the above loss at time t=0 so

$$\left(\frac{d\, n_e}{d\, t} \right)_{dif} = -\, n_e\, \frac{D_a\, 2.4^2}{r^2} \tag{6}$$

A close approximation of D_a is

10

$$D_a = D_i(1 + T_e/T) \qquad (7)$$

[Ref 14:188]

where T_e is the electron temperature, T is the classical gas temperature, and D_i is the ion diffusion coefficient approximated by

$$D_i = \frac{k\,T}{m\,\nu_f}. \qquad (8)$$

[Ref 4:138]

where k is Boltzmann's constant, m is the atomic mass of the diffusing molecule, T is the classical gas temperature and ν_f is the collision frequency of the diffusing ions with the molecules in the gas. The collision frequency is defined by the relation

$$\nu_f = n\, \overline{\sigma\, v_i} \qquad (9)$$

[Ref 4:136]

where n is the density of the gas, σ is the average momentum transfer cross section and v_i is the average thermal velocity of the diffusing species. For CO_2 at $400^\circ K$, $v_i = 3 \times 10^4$ cm/sec. Assuming a momentum transfer cross section of $5 \times 10^{-15} cm^2$ (hard ball sphere approximation) and a pressure of 1 torr, $\nu_f = 4 \times 10^6 \ sec^{-1}$. The resulting D_i is then 190 cm^2/sec which should be

11

representative for the work performed here. For electrons with 2 eV energy, eq (7) yields $D_a = 1.1 \times 10^4$ cm^2/sec.

Attachment Loss

Whenever an electron collides with a neutral molecule, there is a chance that a negative ion will be formed. Attachment will be pronounced where molecules with nearly filled outer electronic shells are present (such as oxygen and chlorine).

For the work presented here, attachment losses are assumed to be minor and will be ignored based on work under similar low pressure conditions in [Ref 25].

Plasma Frequency

The plasma frequency is the cutoff frequency of electromagnetic radiation traveling through a plasma. Any frequency below the plasma frequency is not a solution for a traveling wave and the wave will be attenuated in the plasma [Ref 4:103]. The plasma frequency ω_p is

$$\omega_p = \left(\frac{n_e \, e^2}{m_e \, \epsilon_0} \right)^{1/2} \text{ radians} \tag{10}$$

[Ref 2:5]

where m_e is the mass of the electron and ϵ_0 is the permitivity of free space. After simplification and dividing by 2π to convert into Hz, the plasma frequency can be approximated by

$$f_p \cong 9000 \ (n_e)^{1/2} \ cm^{3/2}\text{-Hz} \qquad (11)$$

where f_p is the plasma frequency in Hz. For electron densities between $6x10^9/cm^3$ and $6x10^{10}$, the plasma frequency limits are 700 MHz to 2.2 GHz.

Because electromagnetic waves at frequencies below the plasma frequency are attenuated, the applied field must exceed the plasma frequency if penetration of the plasma is desired.

Debye Length

Plasmas tend to shield externally applied DC electrical fields from the plasma interior because of redistribution of charge. This characteristic shielding distance, called the debye length, is the approximate distance local variations of charge in a plasma are shielded from the rest of the plasma and is defined by

$$\lambda_D = \left(\frac{K \ T_e}{4 \ \pi \ n_e \ e^2} \right)^{1/2} \qquad (12)$$

[Ref 4:10]

where T_e is the electron temperature. This simplifies to $\lambda_D = 740 \ (kT_e/n_e)^{1/2} \ cm^{-1/2}\text{-eV}^{-1/2}$ if kT_e is expressed in eV. If the dimensions of the system under consideration are much greater than the debye length, the plasma can be considered to be quasi-neutral (ion density≡electron

13

density). For an electron density of $1 \times 10^{10}/cm^3$ and an electron temperature of 2 eV, the resulting debye length is 0.01 cm.

Excitation

In order for a laser to work at all, the proper energy levels of the lasing medium must be excited. Figure 3 shows the fraction of the input power which goes into different types of excitation of a CO_2 laser. High pumping
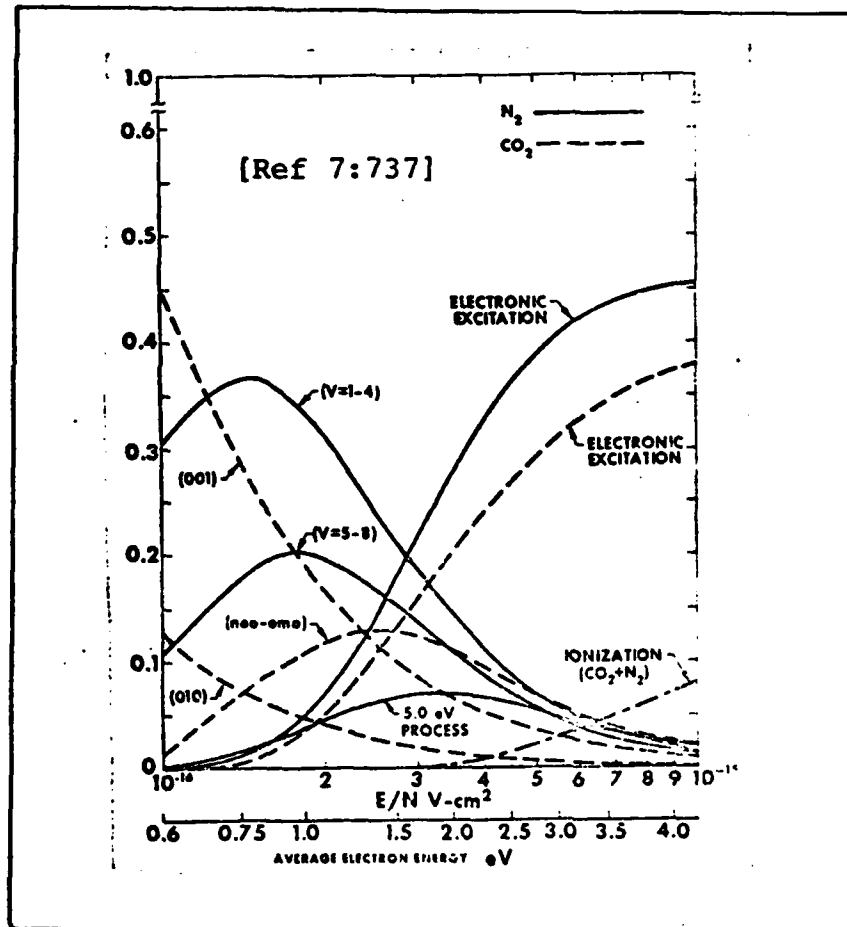

Figure 3. Fractional power transferred from the electrons in a $CO_2$2:N_2:He laser (10:10:80) to CO_2 and N_2 as a function of E/n and average electron energy.

14

rates for the (001) vibrational level of CO_2 and v=1-8 for N_2 are desired (to be covered in Section V). Energy going into electronic excitation is wasted, since that energy does not contribute the population inversion of the desired vibrational energy levels. By necessity, a small amount of the absorbed energy goes into ionization.

Ionization

Without ionization, a discharge could not be self-sustaining. Any electrons present in an initial discharge will be lost because of diffusion, recombination, and attachment. Ionization can take place by direct electron collisions with molecules, atoms, or ions. The electron temperature must be high enough so there is sufficient ionization to maintain the discharge. Otherwise, an external ionization or source of electrons must be used to maintain an electron density.

Figure 3 also shows that optimum excitation of the vibrational levels of CO_2 and N_2 are not obtained if a significant fraction of input energy goes toward ionization. Hill developed a technique of creating a controlled avalanche ionization [Ref 13] using 50-75 nsec high voltage pulses and photoionization to maintain high electron densities. This allows using a separate field with lower E/n ratio for more efficient pumping. The lower E/n ratio results from the electron density increase causing a corresponding increase in the conductivity of the gas.

15

Other auxiliary ionization techniques include the use of X-rays, UV, electron beams, and microwaves. Handy and Brandelik used 2.45 GHz pulsed microwaves in conjunction with a DC discharge to slightly increase the overall efficiency of a small CO_2 laser. While no reason was given for the increase in efficiency, the microwaves were probably of sufficient strength to cause an avalanche ionization. The resulting high electron density reduces the resistance of the plasma. The lowered resistance in turn reduces the electric field in the discharge to lower the E/n ratio, decreasing the velocity of the electrons and improving the efficiency of the DC pumping.

IIb. Microwave Discharges

This section explains some of the differences between the DC and microwave fields. The concepts developed under the DC discharge section also apply here.

Effective Field

Because the microwave radiation is an oscillating field, any free electrons will be accelerated and deccelerated by the alternating E field. An effective E field is given by the expression

$$E_{eff} = E \left(\frac{v_c^2}{v_c^2 + \omega^2} \right)^{1/2} \tag{13}$$

[Ref 20:64]

where E is the applied E field, v_c is the electron-molecule collision frequency/electron and ω is the frequency of the microwave field.

Skin Depth

Much as a distribution of charge in a gas causes debye shielding, a characteristic skin depth is associated with a plasma. This is the characteristic depth an electromagnetic radiation field travels into a plasma before being attenuated by a factor of 1/e. For the work here, the collision frequency of an electron with the gas

is less than both the plasma frequency and the microwave radian frequency.

For $\omega < \omega_p$ (radians), attenuation of an RF signal passing through the plasma is large. The skin depth λ_s is then given by

$$\lambda_s = \frac{c}{\omega_p}\left(1 + \frac{3\nu^2}{8\omega^2} + \frac{\omega^2}{2\omega_p^2}\right) \tag{14}$$

[Ref 12:8]

where c is the speed of light and ω is the frequency of the attenuated radiation. The solution for the attenuated field is $E = E_0 \exp(-x/\lambda_s)$ where E is the magnitude of the attenuated electric field component a distance x in the plasma with an applied field E_0 [Ref 4:103].

If $\omega > \omega_p$ the plasma becomes almost transparent to incident radiation. The skin depth is then given by

$$\lambda_s = \frac{c}{\omega_p}\left(\frac{2\omega^2}{\nu c \omega_p}\right)\left(1 - \frac{\omega_p^2}{\omega^2}\right)^{1/2} \tag{15}$$

[Ref 12:9]

Simplified Model

A simple model will be used to compare the fundamental differences between a longitudinal DC discharge and a microwave discharge as they relate to this experiment.

For a longitudinal DC discharge in a tube, the current

18

must be identical at each point along the tube. The gas
can then be modeled as a series of resistors [Ref Fig 4].
Each resistive element will change resistance so the
current sets a stable operating point on the
voltage/current curve characteristic of this 'gas' [Ref Fig
2].

However, the microwave discharge can be modeled as a
transmission line exhibiting inductance and capacitance.
If energy is taken from the field, at one point along the
transmission line, less energy is available to transmitted
to the rest of the line. Local boundary conditions can
induce higher fields into one particular region of gas,
causing higher local currents in one region over another.
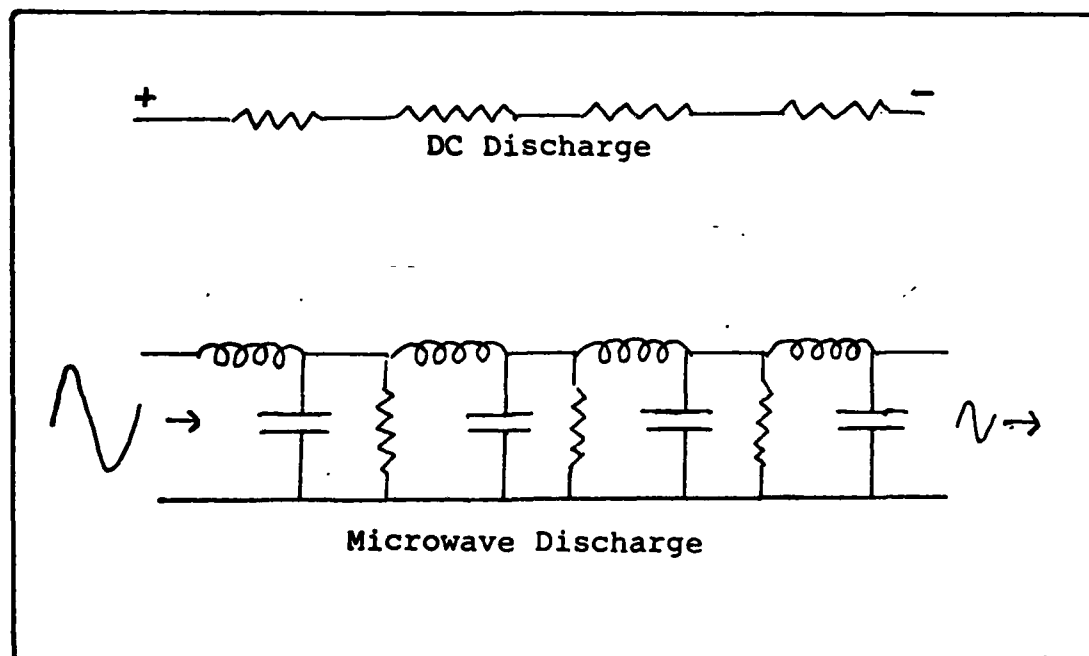If the current causes a localized discharge in one region

Figure 4. Simple Discharge Model.

of the tube, enough power can be absorbed to prevent any type of discharge from occurring further down the line.

Electron Density in Microwave Fields

Because of the skin depth effects, microwave fields are shielded from the plasma interior. Diffusion depletes the electron density near the wall of the tube. In pulsed microwave discharges in a cylindrical tube, the greatest concentration of electrons is concentric to and concentrated near the walls. Vasyutinskii examined this while looking at pulsed microwave laser pumping [Ref 25]. An earlier work [Ref 1] discusses electron density in high frequency discharges between parallel flat electrodes with similar results, only in planar symmetry.

Because the microwaves are shielded from the interior part of the plasma, the core electron density is controlled by diffusion from the ionization skin. Since attachment and recombination losses are believed to be insignificant, the core electron density in the CW discharges will increase to almost the same density as that in the ionization region near the tube wall.

An estimate of the upper limit of the electron density generated by a microwave discharge is made by setting the plasma frequency equal to the microwave frequency, 2.45 GHz here, in equation (11) and solving for the resultant electron density. This yields an approximate upper limit of 7.4×10^{10} cm^{-3}.

20

III. CO_2 Laser

The CO_2 laser is a four-level laser with a quantum efficiency of 45%. While pure CO_2 can be made to lase, the addition of gases, such as N_2 and He, are used to alter the electron and heavy particle kinetics. For optimized mixes, actual efficiencies achieved approach 27% [Ref 5:281].

Development of this section will include a brief description of the CO_2 vibrational modes. Next will be a summary of the energy levels of CO_2 relevant to lasing and the role of gases such as N_2 and He in the lasing process.

CO_2 Molecule

The CO_2 molecule is linear and symmetrical. There are three normal modes of vibration, symmetric stretch (v_1), bending (v_2), and asymmetric stretch (v_3) [Ref Figure 5]. The vibrational states will be referenced in the standard form of ($v_1 v_2 v_3$).

The normal lasing transition for the 10.4 micron band in CO_2 is from the asymmetric stretch mode (001) to either the bending mode (020) or the symmetric stretch mode (100). If the transition is to level (020), lasing is in the 9.4 micron band. If the transition is to the level (100), lasing is in the 10.4 micron band [Ref Fig 5].
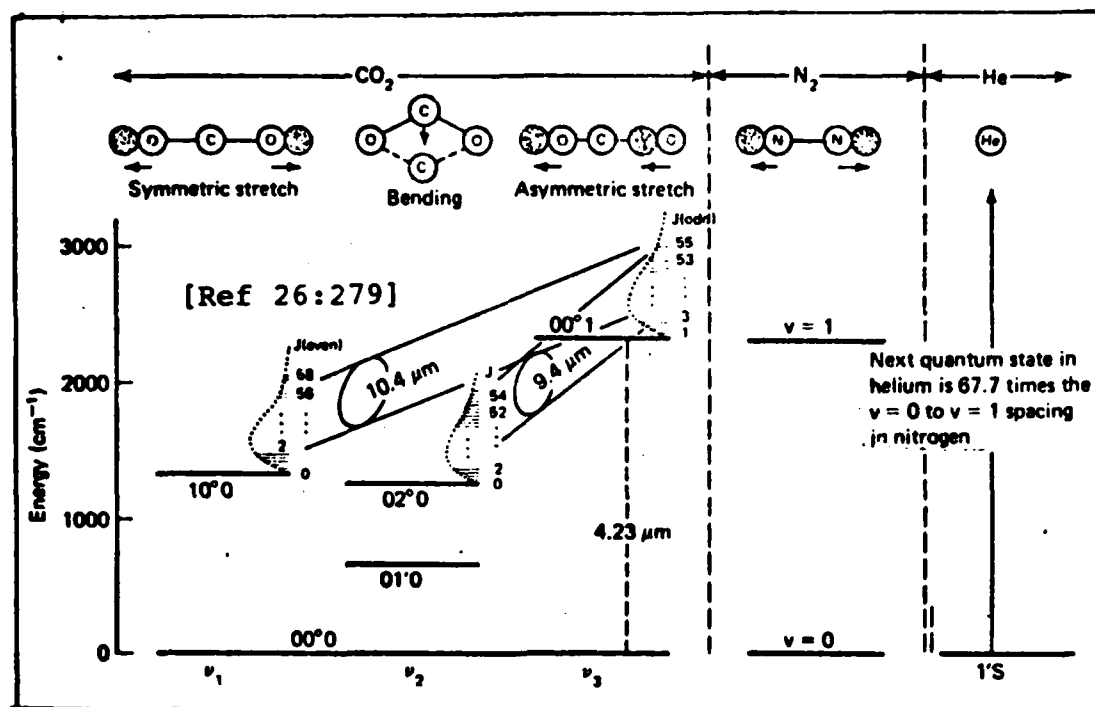
Figure 5. Energy level diagram for CO_2:He:N_2 Laser.

Besides the vibrational transitions, there is a simultaneous change by one in the rotational quantum number. The combined vibration-rotation spectrum allows approximately 200 lasing transitions from 9-18 microns.

Addition of Nitrogen

The v=1 vibrational energy level of N_2 is only 18 cm^{-1} from the (001) upper laser level of CO_2. Nitrogen has a larger cross section to the exciting electrons for vibrational levels v=1 to 8 than CO_2 has for the (001) upper laser level. Thermal energy from the gas is sufficient to allow resonant energy transfer from the N_2 to the CO_2.

Nitrogen is able to store this energy for long periods

of time because it is a homonuclear molecule. Vibrational energy cannot induce a dipole in N_2 so that radiative transitions are forbidden [Ref 5:278]. Virtually all the energy stored by N_2 in this metastable state can be transferred to the desired upper laser level in CO_2. At room temperature, this characteristic transfer time is

$$\tau_{vv} = (n_N^* \ 4 \times 10^{-13} \ cm^3 \ sec^{-1})^{-1} \qquad (16)$$

[Ref 8:12]

where n_N^* is the density of vibrationally excited N_2. At a pressure of 1 torr with a 10% gas concentration of N_2 where 20% are vibrationally excited, $\tau_{vv} = 5 \times 10^{-3}$ sec.

Addition of Helium

Helium is also used in the CO_2 laser to improve efficiency. The primary role of He is to depopulate the (010) level of CO_2 [Ref 18:20]. He is more than 10 times as effective in depopulating the (010) level than are N_2 and CO_2. However, He also alters the energy distribution of the electrons and helps conduct heat from the plasma to the tube wall.

Resonator Design

Feedback must be provided to get oscillation. The design must be so that losses are kept low. At the same time the mode volume should be large so that the excited molecules can contribute to the photon field by stimulated emission.

For oscillation to occur, gain must equal losses. In practice, the small signal gain will be slightly larger than the loss, but the laser saturates in oscillation and the gain is reduced to exactly equal the losses.

Often, two curved or one curved and one flat mirror are used to make the laser resonator. Proper selection of the radius of curvature can make alignment less critical and establish the desired mode volume and spot sizes.

A resonator has a Gaussian solution if the condition $0 < G_1 G_2 < 1$ is satisfied where $G_i = (1 - L/R_i)$. The term L is the separation between the two mirrors of the cavity and R_i is the radius of curvature of the mirror. The development of the solution of a stable resonator is straightforward but tedius by using the matrix method and is included in Appendix A. The desired results are summarized here. The waist size, the radius of the beam where it is most narrow, is found from the expression

$$W_0 = \left[\left(\frac{Y\ L}{\pi\ (G_1 + G_2 - 2G_1G_2)} \right) \left[(G_1 G_2) (1 - G_1 G_2) \right]^{1/2} \right]^{1/2} \tag{17}$$

[Ref eq (A-38)]

where Y is the wavelength of the light in the cavity. The location of the waist is given by

$$z_0 = \frac{L(1 - G_1)(G_2)}{(G_1 + G_2 - 2G_1G_2)} \qquad (18)$$

[Ref eq (A-32)]

The beam size at any location in the cavity can now be calculated from the above parameters by

$$W = \left(\frac{Y}{\pi}\right) \left(\frac{(Z-Z_0)^2 + Q_0^2}{Q0}\right)^{1/2} \qquad (19)$$

[Ref eq (A-43)]

where Z is the location for finding the spot size, and $Q_0 = (\pi W_0^2/Y)$.

IV. Equipment

This section gives a brief description of the equipment used in the experiments for this research. Emphasis will be placed on unique equipment, especially the microwave irradiation apparatus, mixing manifold, and vacuum manifold. Commercially available monitoring equipment which is generic in nature will not be described.

The microwave irradiation facility provides a versatile and efficient means of applying both CW and pulsed microwave energy in the 2.45 GHz band. The system consists of two almost identical applicator systems to provide a uniform microwave energy field to a small cross section over a length of 46.5 cm. All sources are isolated from each other by various microwave devices so that any combination of sources can be operated without mutual interference.

Microwave Sources

The two CW microwave sources used in this experiment are Gerling Moore, Inc. Model 4006. They can provide 2.5 kilowatts of low-ripple microwave energy at 2.45 GHz. Microwave energy from the sources is transmitted through waveguide connections. The units are operated at approximately 80% full power to minimize ripple.

Pulsed microwave power is available from two Epsco Model PG5KB generators. Each is capable of

generating a peak output of about 4.5 kilowatts. Tuning is possible over a range of 2.35 to 2.7 GHz. While these units have internal triggering available, the external synchronization input was used to have precise control of the timing of the two units. Pulse widths are provided in two ranges from 0.3 to 50 microseconds. Power output from these sources is made through a coaxial cable. The power is transfered into the waveguides using a coaxial cable-waveguide interface.

Microwave Applicators

Microwave energy is coupled into the discharge tubes with the use of two Gerling-Moore, Inc. Model 4055 interdigital slow wave transmission lines [Ref Fig 6]. The applicator consists of a channel milled 3.3 cm deep in the metal stock.

Microwave energy is fed into one end of the channel. As microwave energy is transmitted through the transmission lines, an evanescent field is present which can interact with the gas in the discharge tube. The active surface is 4 cm by 46.5 cm. The applicators are rated for a maximum of 3 kW. The manufacturer specifications list a field strength of 5000 volts/cm at the surface with an input of 2.5 kW. The field falls off exponentially and becomes insignificant at about 10 cm above the applicator in the free space configuration. The electric field 1.5 cm above the surface of the applicator is about 0.5 the electric field at the surface.
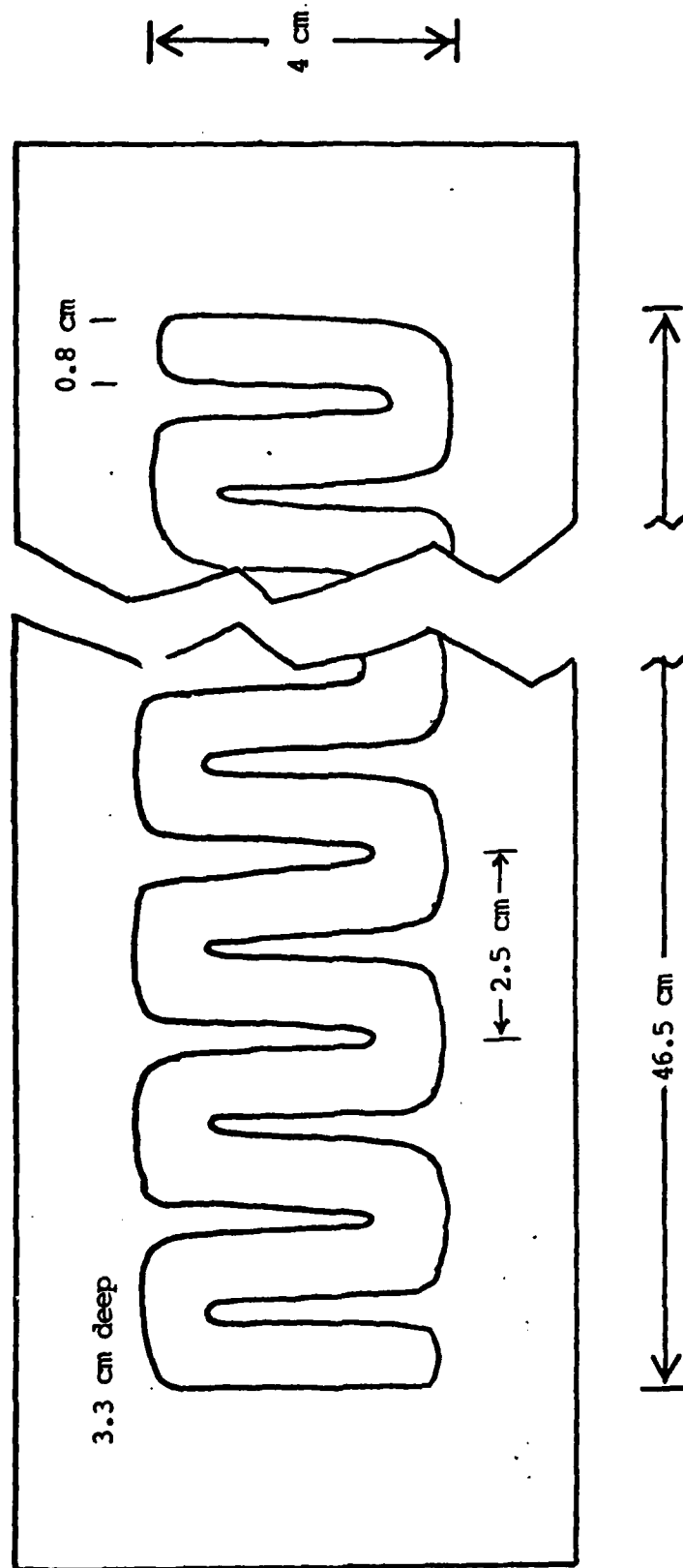
27

Figure 6. Surface of microwave applicator.

28

With two applicators making a sandwich in close proximity, boundary conditions are imposed and the field structure can be expected to be different from the free-space configuration.

Because the applicator is a transmission line, any power absorbed along the line will decrease the power available further down the line. The evanescent wave contains part of the total energy of the transmission line. Any absorption of the evanescent wave is a reduction of the total remaining energy traveling in the applicator. This effect can cause some discharges to be highly non-uniform, which is very gas dependent. This effect was a major obstacle in getting a uniform discharge in He which had more than a few percent concentration of molecular gases (specifically CO_2 and N_2). Tilting the tube between the two applicators minimized the problem enough for other experiments [Ref 23:59], but was not the solution in this work.

Microwave Components

Various microwave components are used to control the microwave energy and to deliver the energy to the applicators. Three-stub tuners are used to direct the desired amount of RF radiation to the applicators. Dummy loads are used to absorb the unwanted energy. Circulators are used in conjunction with the dummy loads and tuners to isolate the microwave sources from each other and prevent damage from reflected radiation.

The basic configuration of the microwave system is shown in Figure 7. This configuration was used throughout all the experiments in this work.

Protection circulators allow energy transmitted by each of the sources to bypass a dummy load and be transmitted to the applicators. However, waste microwave energy coming toward a source gets diverted to a load to prevent damage to the sources. Another circulator, three-stub tuner, and dummy load system on each of the CW sources are used to attenuate the transmitted radiation. The three-stub tuners are inserted to permit some of the incident radiation to be reflected back through the waveguide network into the applicators. The CW power is adjusted with the tuners so the power from the sources can be kept constant to minimize ripple.

Directional power is measured with the use of Hewlet-Packard model 420 crystal detectors. These units were calibrated in 1982 and were not calibrated again for this work. Accuracy of 5% is claimed by the manufacturer when the crystals are properly calibrated, however, they are susceptible to mechanical shock and high transient voltages (as can be encountered by a tesla coil, often required to initiate a discharge).

The applicators are connected to the rest of the microwave system using flexible waveguides and quick connect clamps. This allows for easier reconfiguration or mechanical relocation of components.
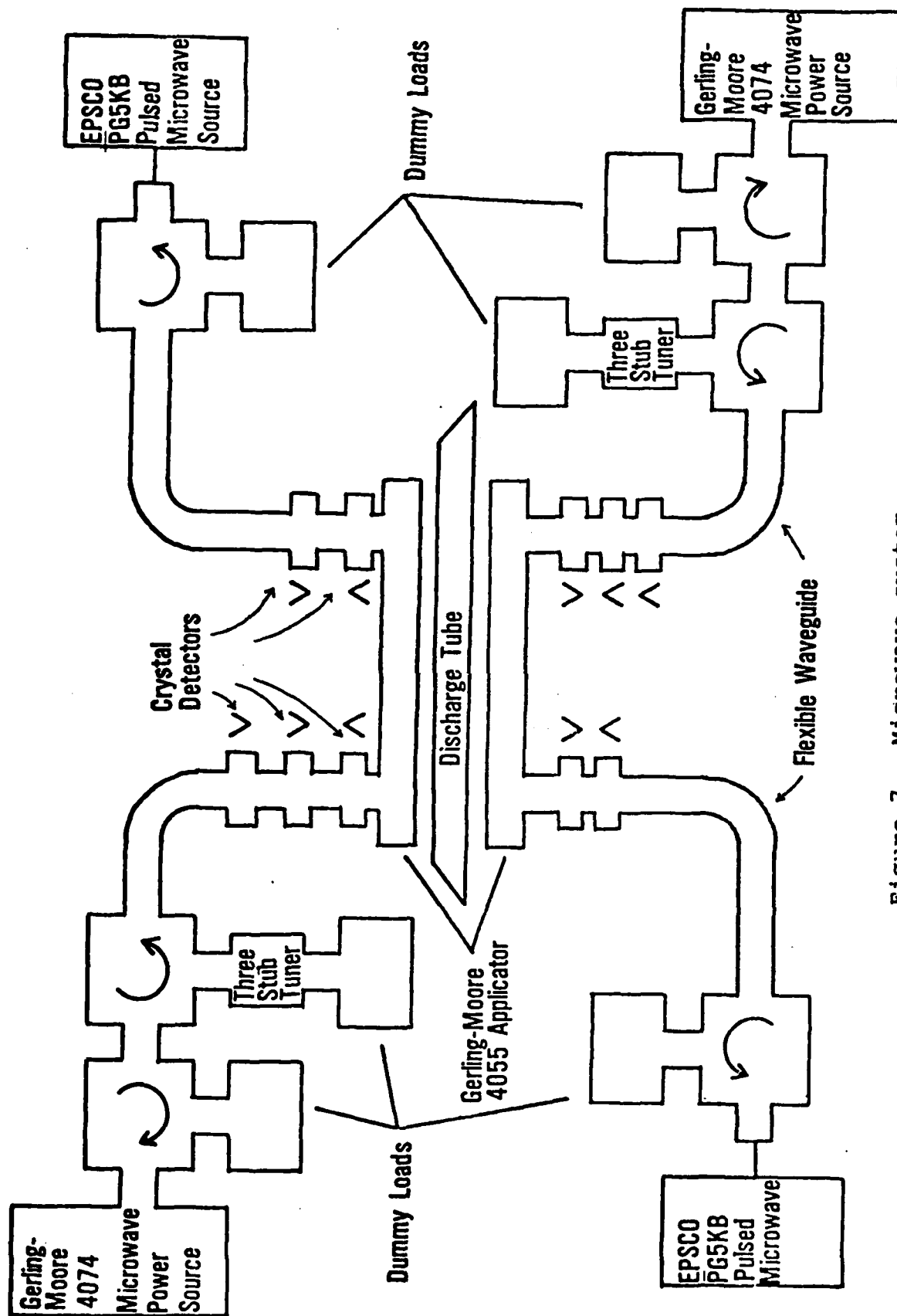
Figure 7. Microwave system.

Safety Equipment

A number of safety features are included in the system to protect both personnel and equipment.

A Holiday Industries, Inc. Model HI-1500-3 microwave interlock system is the major personnel protection device. If ambient microwave power in the area becomes excessive, all microwave power will be shut down.

A mechanical push button is connected to the HI-1500-3 interlock. Pushing this button activates the shut-down of the microwave power sources in the same manner as the automatic shutdown.

A portable microwave field intensity meter is used as an added precaution. Whenever equipment configurations were changed, microwave power levels were monitored on a system startup to ensure that excessive microwave radiation did not leak into the room.

DC Power Supply

A controllable 0-5 kilovolt power supply was used in this experiment to establish a baseline laser output level.

The power supply circuit used is shown in Figure 8. It consists of a Spellman power supply which allows control of voltage or current output, a ballast resistor, and sensing resistors. Because the current anticipated for establishing lasing was less than 10 ma, the ballast resistor network was chosen to limit the current with more control than is available with the power supply. The
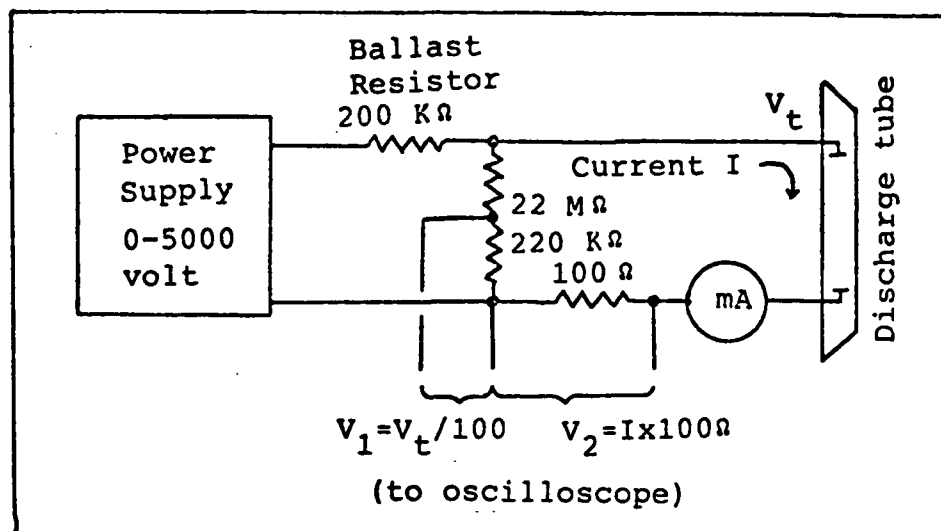
32

Figure 8. Power supply Ballast and sensing network.

ballast consists of two 400 kilohm ceramic power resistors connected in parallel to result in a 200 kilohm resistance.

The sensing resistors allow the tube voltage and tube current to be monitored simultaneously on a multi-channel oscilloscope. A Simpson Model 260 multimeter on the 10 milliampere scale was also used to monitor DC current through the discharge tube.

Discharge Tubes

Three different discharge tubes [Ref Figs 9,10,11] were used in this experiment. The first two had limited usefulness due to mechanical failure. The third was the source of most of the data in this set of experiments. All tubes were made from quartz because of quartz's low attenuation of 2.45 GHz microwave radiation.

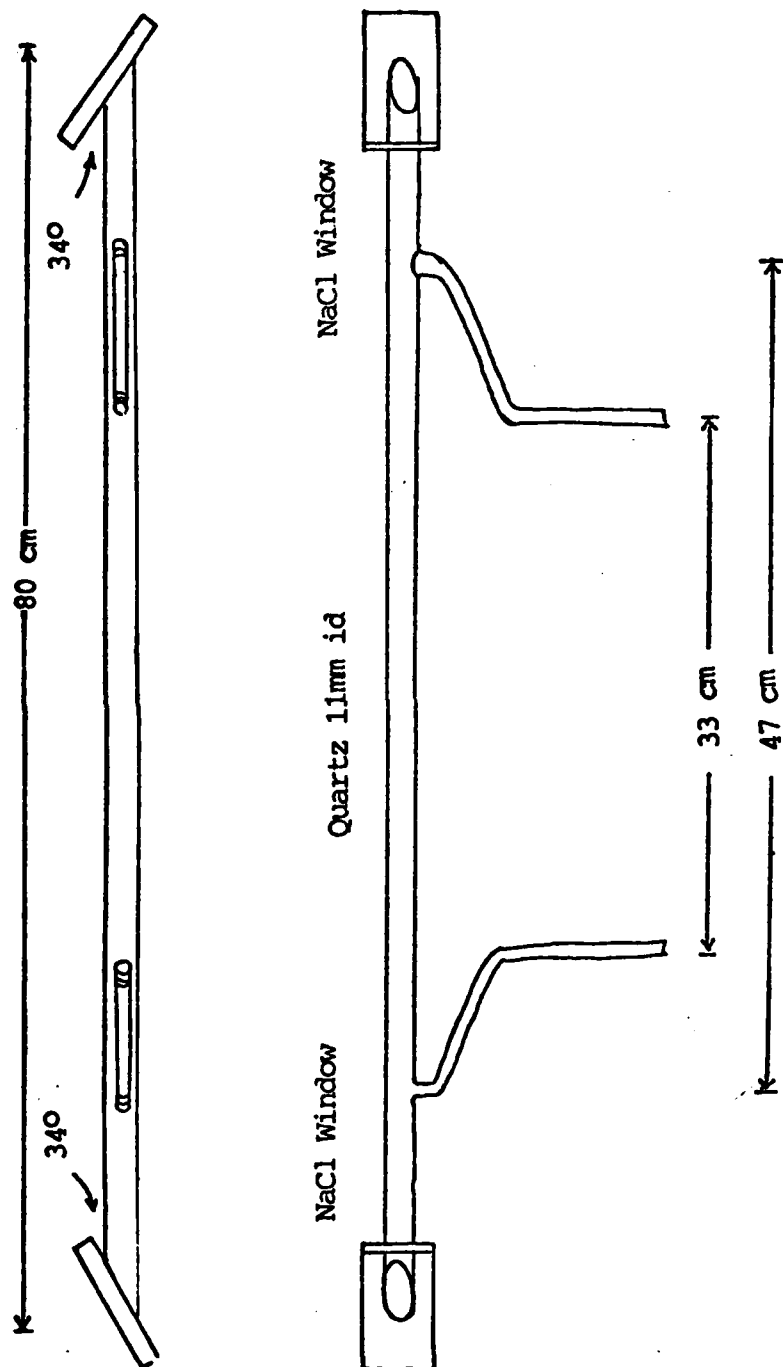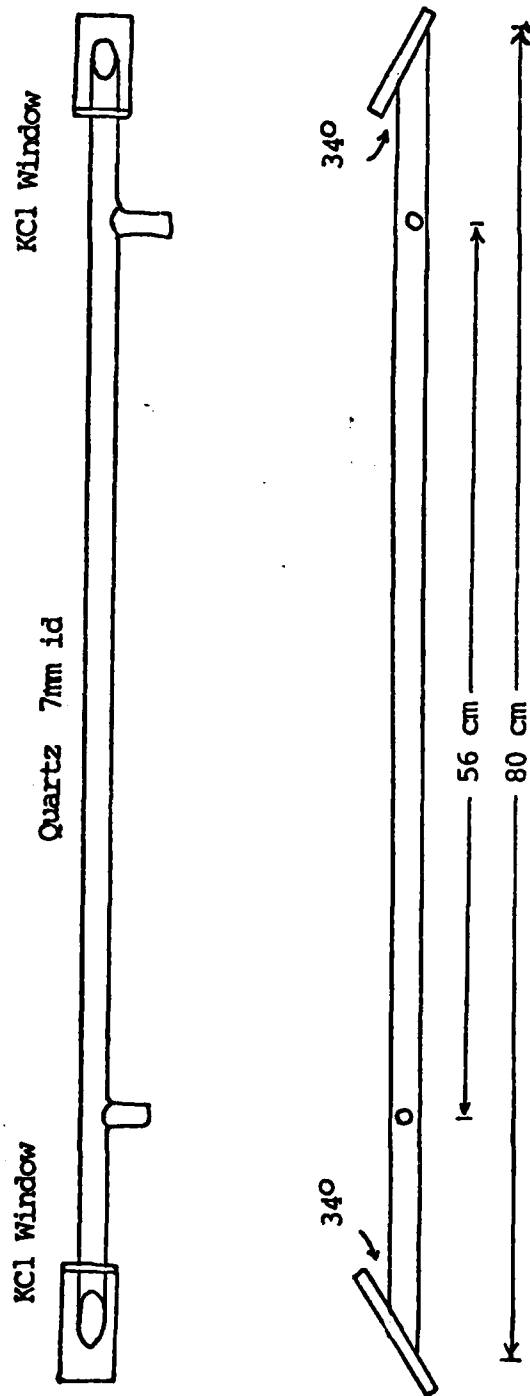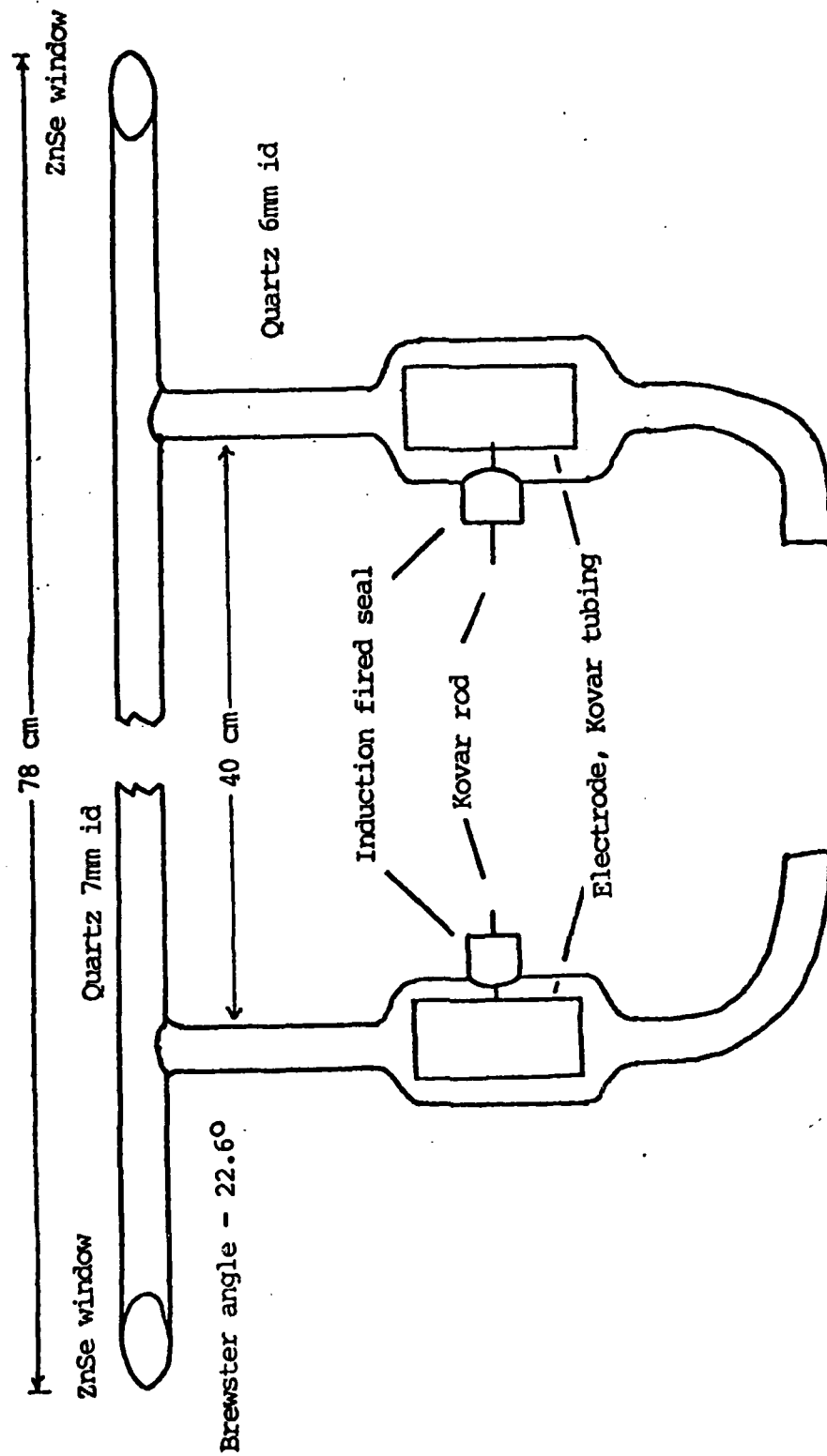Figure 9. Discharge tube #1.

34

Figure 10. Discharge tube #2.

35

ZnSe window

Quartz 6mm id

78 cm

40 cm

Quartz 7mm id

Induction fired seal

Kovar rod

Electrode, Kovar tubing

Brewster angle – 22.6°

ZnSe window

Figure 11. Discharge tube #3.

The first tube was designed with NaCl windows at the Brewster angle for 10.6 micron IR (33.7° relative to the beam). The value for the index of refraction used was 1.5. This tube was broken while attempting to correct a binding problem on one of the microwave applicators shortly after the tube was installed in the system.

Tube #2 was basically the same as the first tube with the exception of shorter gas connection arms. Windows for this tube were KCl (index of refraction = 1.46 at 10.6 microns) set at the Brewster angle, 34.4° (relative to the beam direction). This tube was used in a number of experimental attempts to get lasing using only CW microwaves as the pumping source. The lack of success led to development of a gain measurement technique and to the design of tube #3. Tube #2 also had a limited lifetime due to cracking and leakage of one of the Brewster windows.

Tube #3 was designed with electrodes so lasing could be attempted using a DC pumping scheme. Because of the physical constraints of the applicator system, the electrodes were placed in the gas inlet/outlet sidearms to allow more flexibility in tube placement within the microwave applicator structure. The gas inlet/outlet arms were made with larger diameter tubing (6 mm id) so that gas viscosity effects could be reduced.

Initial estimates were the tube would have to dissipate a maximum of 30 watts. Two identical electrodes consisting of Kovar tubing 5 cm long x 1 cm diameter with

37

0.1 cm thick walls were tapped and connected to small Kovar
rods which acted as the electrical feed-throughs. The
feed-throughs were substrated into the quartz tubing using
an induction firing process.

Gas Manifold System

Two basic gas manifold systems were used in this work.
Both were used in the flowing-gas mode of operation to
maintain gas purity and to provide additional cooling of
the laser mixtures. The first manifold allowed for
introduction of only one gas into the discharge tube. The
second manifold allowed for real time mixing of three gases
with a capability of expanding to six.

The basic one-gas manifold system was used during
initial observations of discharges.

The three-gas mixing approach [Ref Fig 12] was chosen
because it was felt that the gas mixture to achieve lasing
using the CW microwaves would have to be carefully
regulated. The manifold consists of six quick-release
valves and six needle valves (only those used are shown for
clarity). The individual gases are fed into a chamber
filled with glass beads to provide mixing of the gases. No
other specifications are available on this manifold.

The flow of the gases was monitored by Hastings mass
flowmeters. Calibration was accomplished by timing how
long it takes a soap film to travel up through a graduated
cylinder. Corrections were made for temperature, air
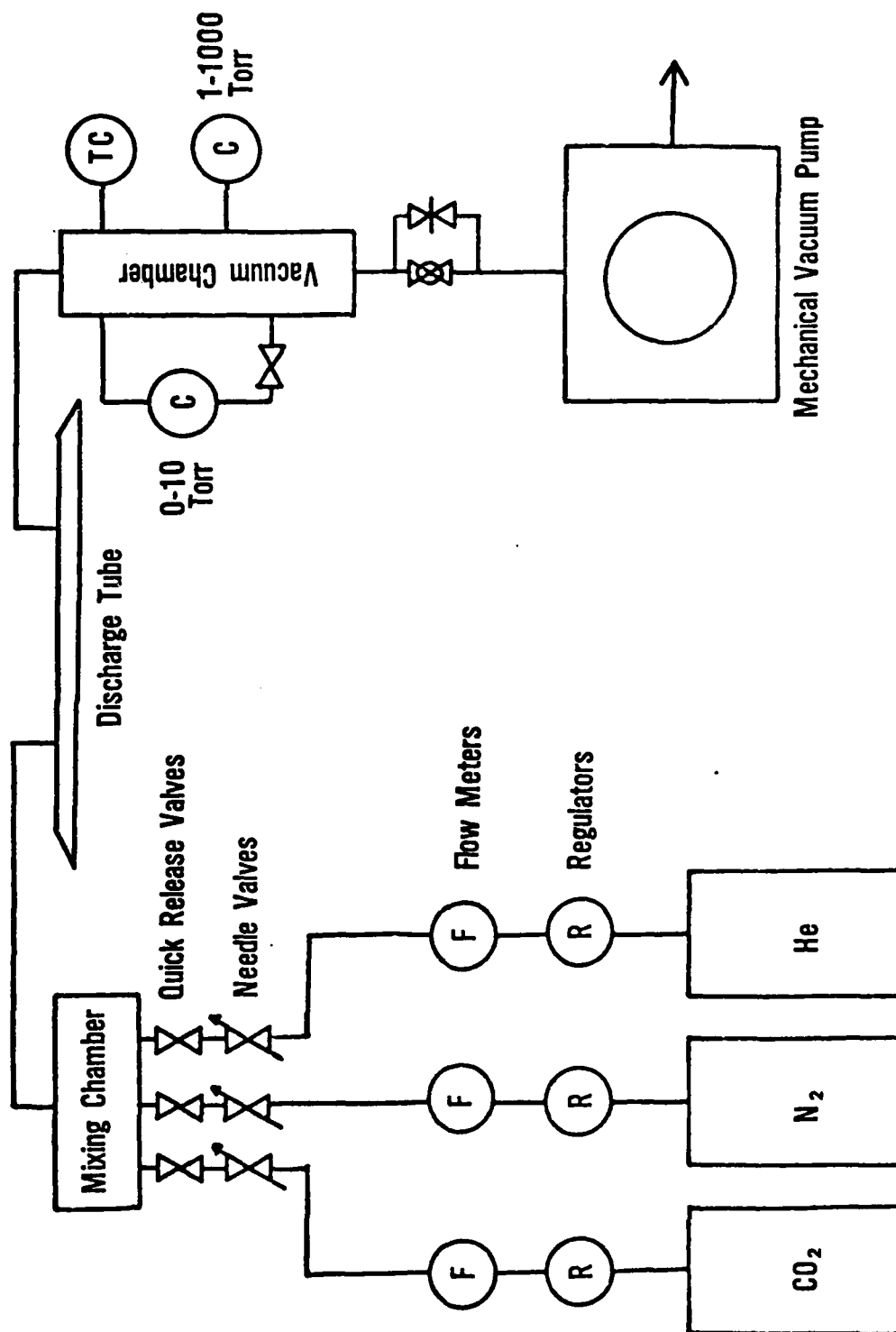pressure, and water vapor pressure.

38

Figure 12. Gas-vacuum system.

39

Vacuum System

Vacuum was provided by two basic vacuum manifold systems. Once again, the first was used in the early stages to get a feel for modifications necessary for later work.

The second design [Ref Fig 12] was chosen to reduce conductance for high flow rates. The main feature of the second design was shorter connecting lines from the vacuum pump to the discharge tube. Two MKS Baratron pressure sensors, MKS Model 220BHS-4A-B-1000 (0-1000 torr) and MKS Model 315BH-10 (0-10 torr) were used to measure the pressure in the vacuum tank. The 0-1000 torr sensor requires a 24 V input and provides an output of 0.01 volts/torr which can be read on a digital voltmeter.

The 0-1000 torr gauge was used primarily to determine when the discharge tube system could be safely handled and opened to atmospheric pressure. The 0-10 torr gauge had a reference vacuum connection which necessitated having another vacuum gauge to determine when the best vacuum was attained. A Hastings DV-6M vacuum sensor gauge provided this information and all pressure readings are made from the minimum attainable from the vacuum pump.

IR DETECTORS

Several types of detectors were used in the detection of pulsed and modulated infrared radiation: pyrolectric, thermopile power meter, and cryogenically cooled photoconductive.

40

Two pyroelectric detectors were available, one a Molectron model P3 detector which provides three settings of speed/sensitivity. The other detector was of unknown origin, but had characteristics similar to the high sensitivity setting of the Molectron P3 detector with slightly better response time.

Pyroelectric detectors require a chopped signal. The output signal is nearly proportional to the input signal after the transients have damped out. No specific calibration of the pyroelectric detectors is required. The Molectron unit is battery operated only.

A Scientech Model 262 power meter was used to measure laser output power. The unit operates on the thermopile principle, consequently, useful for looking only at average power in pulses or steady state power. The smallest detectable signal is about 10^{-5} watts.

A Santa Barbara Hg:Cd:Te detector was used to look at fast transients of the laser output. The unit is cryogenically cooled. Even with outputs of 50 mw, the laser beam had to be attenuated by about three orders of magnitude to keep from saturating the detector.

Gain Measurement Apparatus

The method for measuring gain developed here [Ref Fig 13] compensates for the fluctuating output of the probe laser.

The probe laser is a Laakman model RF44 waveguide laser with a nominal output of 5 watts. The probe laser was
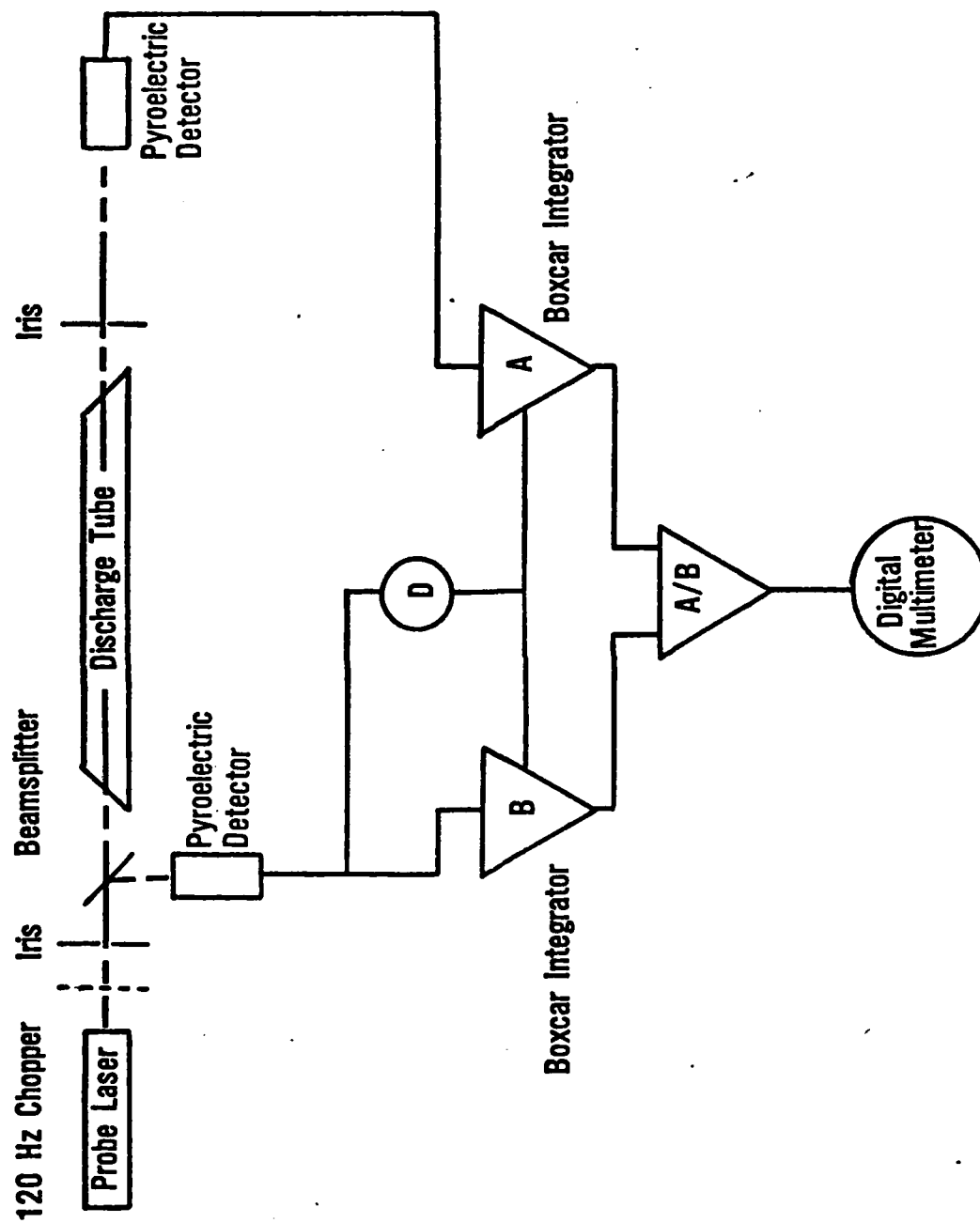
41

Figure 13. Gain measurement apparatus.

42

placed about 4 meters from the discharge tube so divergence
reduced the power to an estimated 10 mw available in the
probe beam. A 120 Hz chopping wheel provides the necessary
modulation for the pyroelectric detectors.

An iris with about a 3mm opening was placed at one end
of the discharge tube and another at the other end to help
mask reflections from the tube walls due to diffraction. A
beam splitter was placed between the first iris and the
discharge tube to direct a portion of the probe beam to a
pyroelectric detector for a reference signal. The second
pyroelectric detector is used to provide the measurement
signal to be compared against the reference signal.

The two signals were fed into two similar boxcar
detectors (PAR model CW-1 and PAR model 160) used as gated
integrating amplifiers. The probe reference signal was fed
into the model 160 boxcar integrator. The gate signal from
the model 160 was used to gate the amplifiers on both
integrators. The outputs were fed into an analog divider
so the magnitude of the probe signal is divided into the
other. A 3-1/2 digit multimeter was used to display the
result.

Gain can be measured by first obtaining a no-gain
reading of A/B (where A is the signal from the probe beam
traveling through the discharge tube and B is the reference
signal). A discharge is then established in the laser gas
mixture and a reading of A'/B is then recorded, where A'
is the probe signal through the discharge tube which will

43

be amplified if there is gain. Gain is then $(A'/A - 1)$
or (by using the two readings), $((A'/B)(B/A) - 1)$.

V. Experimental Results

Resonators

Eqs (17,18,19) aided resonator design. The formulas were written into a computer program as a general aid in designing stable resonator cavities. Appendix B contains a listing of the program converted into standard Microsoft (registered trademark of Microsoft, Inc.) BASIC.

Based on these formulas and the available optics, two cavities were designed [Ref Fig 14]. The first had a 2.5 m radius of curvature for both mirrors with a separation of 1.04 m. Physical constraints of the microwave equipment prevented the use of cavities much shorter than this.
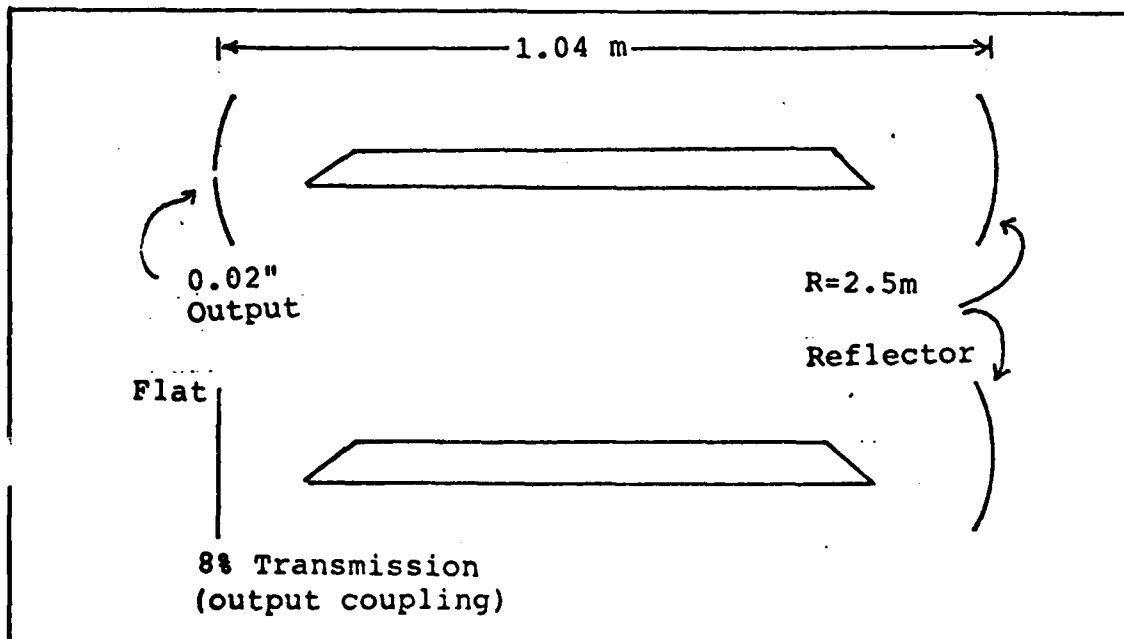

Figure 14. Resonator cavities.

Output coupling of the first resonator was through a 0.02 inch hole in the center of one of the curved mirrors. While technically this is not the classical stable cavity, the perturbation from the hole should not affect the beam significantly. Based on the spot size at the mirror, calculated to have a 2.1 mm radius, output coupling is estimated to be 1.5% by comparing the output area to the spot size at the mirror.

The second cavity consisted of one total reflector of 2.5m radius of curvature and a flat transmissive output coupler with a cavity length of 1 m. This configuration was a true stable resonator. Transmission of the flat output coupler was 8%, according to manufacturer's specifications.

After the cavity parameters were determined, discharge tube #1 was constructed [Ref Fig 9]. As noted previously, tubes #1 and #2 had limited lifetimes so most of the data and observations in the following section are from tube #3 [Ref Fig 11].

CW Microwave Discharge

The original approach was to try to get lasing using CW microwaves as the sole ionization and pumping source. A discharge in a laser mixture consisting of 12% CO_2, 16% N_2, and 72% He (12:16:72) was established in discharge tube #2 at pressures between 0.1 and 1.1 torr. With applied CW microwave power up to 200 watts, the discharge tended to remain localized in small regions of the tube. Shifting

46

the lateral position of the upper microwave applicator, tilting the applicator, and tilting the discharge tube helped only slightly in making the discharge more uniform. The plasma also absorbed most of the incident radiation, in excess of 90%. At powers above 200 watts, discharge tended to become uniform, with most of the incident power again absorbed by the plasma.

Repeated attempts to get lasing with applied CW microwaves at various power inputs resulted with no apparent lasing. Failure to achieve lasing could be due to a number of factors such as excessive loss (defective windows or faulty mirrors), insufficient gain (bad laser mix, low pressure of laser mix, heating of the laser mix, dissociation, contamination), misalignment of the cavity mirrors, etc.

The gain apparatus was used to see how much gain, if any, was available using the CW microwave discharge. No apparent gain was observed at various pressures and power input levels. Results were inconclusive, however, because of polarization instability of the probe beam. The equipment was designed to accomodate fluctuations in power output only.

Discharge tube #3 was used to establish a DC discharge. Measurements yielded single pass gain values of 10-11% with the same laser mix which failed to produce gain in the CW microwave discharge.

DC Pumping

Lasing was established in discharge tube #3 using a laser cavity consisting of two 2.5 m radius of curvature mirrors spaced 1.04 m apart. Supply potential was 5 kV with a 200,000 ohm ballast resistor. The gas mixture was optimized to 7:6:87 (CO_2:He:N_2) at 1 torr. Current through the tube was 6 ma and produced 9 mw of laser power. The low power had to be contended with throughout all work in the remaining experiments. Vibration isolation and gas mixture adjustments did bring the output up to 25 mw, still less than expected. The tube potential was 3.8 kV so total power into the discharge tube was 23 watts. Assuming 10% efficiency, common in CO_2 lasers, about 2 watts out would seem reasonable.

In the initial design, it was determined there would not be severe loss due to diffraction. However, kinetics of the CO_2 laser favor a partial pressure of CO_2 when the relation pD=2 torr-cm is satisfied, where p is the partial pressure of CO_2 and D is the tube diameter [Ref 5:173]. In a parametric study by Rensch, output in a 10 torr CO_2 laser dropped drastically as the tube diameter was reduced to 1 cm [Ref 21:46].

To examine the problem a little further, the electron density and ultimately the operating regime can be obtained. The simplest method is to take an estimate of the gas density and potential across the discharge tube to find the E/n ratio. Fig 3 can then be used to get the

48

approximate fractional amounts of input power going into ionization and the different types of excitation. However, the pressure is not known exactly because of the viscosity effects (which were ignored) and the temperature is only a guess.

For a starting point, the gas is assumed to be $400^\circ K$ at 1 torr. The discharge length is 100 cm and a 200 V cathode fall region is assumed. Computing n from the ideal gas law, this yields an initial E/n value of 1.5×10^{-15} $V\text{-}cm^2$.

A self-consistent value of E/n was determined through a graphical iteration based on establishing the fractional power invested in ionization. The power density going into ionization is given by $P_{ion} = n_e \langle I + \bar{e} \rangle R_i$, where I is the ionization potential, $\bar{e}$ the electron mean energy, and R_i the single particle ionization rate. Because diffusion is the dominant loss mechanism, the ionization rate must equal the diffusion loss rate in a steady state. Thus $D_a / \Lambda^2 = R_i$, where D_a is given by eq (7) and $\Lambda = 0.35$ cm/2.4 . Therefore, the power density going into ionization may be expressed as $P_{ion} = n_e \langle I + \bar{e} \rangle D_a / \Lambda^2$.

The electron density, n_e, is related to the current density and drift velocity according to equation (3). Upon substitution for n_e, this yields $P_{ion} = (J/e \, v_{de}) \langle I + \bar{e} \rangle (D_a / \Lambda^2)$. Here the current density is experimentally determined; whereas v_d and D_a, and consequently P_{ion} are functions of E/n whose dependence is
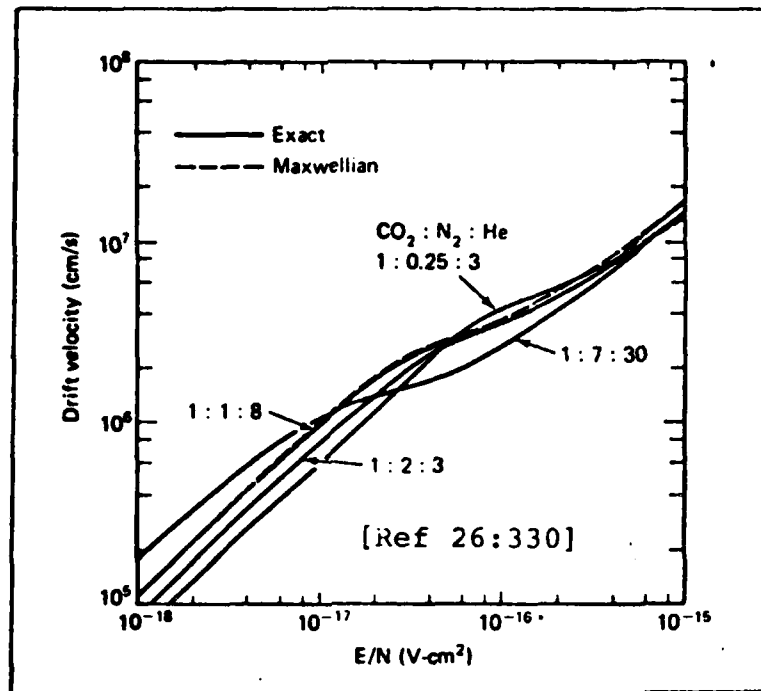
49

Figure 15. Calculated electron drift
velocities for CO_2:N_2:He Lasers.

established using Figs (15 & 3) and eq (6). This equation
forms the basis for the following iteration.

Based on an initial estimate of E/n, the corresponding
drift velocity {Fig (15)} and mean energy {Fig (3)} were
determined. The electron density was then obtained using
eq (3) and the diffusion loss rate established from eq (6).
The total power into ionization, $P_{ion-tot}$ was obtained by
multiplying P_{ion} by the discharge volume. The fractional
power into ionization was then calculated by dividing
$P_{ion-tot}$ by the power input to the discharge. Using the
ionization curve of Fig (3), a new E/n value was
determined. The iteration proceeds to convergence, based
on the updated values of E/n.

50

Starting with the E/n ratio of 1.5×10^{-15} V-cm^2, this iterative, self consistent solution yielded an E/n of 6×10^{-16} V-cm^2. At this value of E/n, 2% of the input power directly excites the upper laser level and another 7% excites the v=1-4 states of N_2. Under these conditions, a maximum of 2 watts pumping power for the upper laser level is available, ignoring all competing depopulating processes. Based on the ·45% quantum efficiency of the lasing process, 0.9 watts is established as the upper limit for laser output.

Pulsed Microwave Pumping

Lasing was established using the above DC pumping conditions. Microwave radiation pulsed at 200 Hz with 10 usec pulse widths from both sources was applied to the discharge. The DC potential was gradually reduced. The upper applicator was tilted so that coupling was improved. Continual adjustments were made to the gas mixture and flow to optimize the laser output as the DC power was reduced.

After the DC supply was turned off, the gas optimization process was repeated and the power of one of the pulsed microwave sources was gradually turned off to establish lasing with only one pulsed source. The laser output was monitored using a pyroelectric detector. The final gas mixture was 14:12:74 at 3.2 torr with a flow of 350 SCCM.

Pulse widths of the microwave radiation were changed to examine the effect on laser output power [Ref Fig 16].
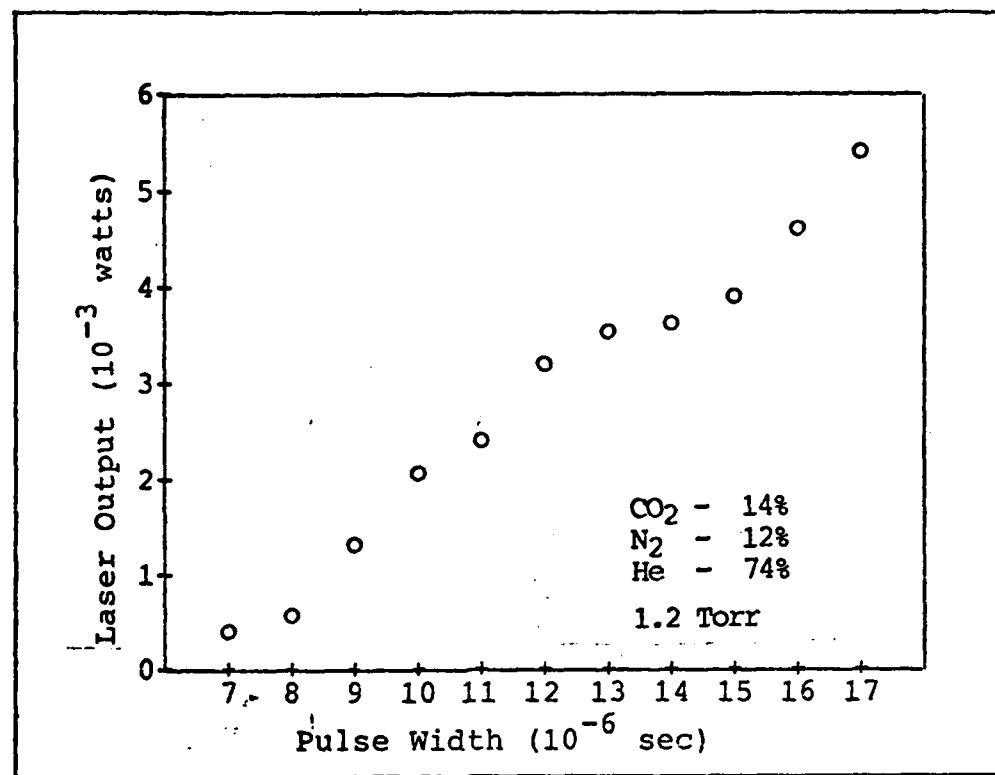
51

Figure 16. Laser power output of a pulse microwave pumped CO_2 laser as a function of the microwave input pulse width.

The laser did not begin oscillation until after the microwave pulse ended. Depending on the power input, alignment of the mirrors and gas mixture, this delay can be more than 100 usec. The delay time is the time it takes to obtain the critical population inversion. Mirror alignment has an effect because losses can be increased if the laser beam is not directed through the center of the laser tube.

Fig 17 shows the results of the laser pulse output delay measured from the start of the applied microwave pulses.

With the pulsed microwaves pump scheme, the laser output consisted of a peaked pulse about 2 usec long followed by rapid decay [Ref Fig 18]. A secondary laser pulse can be seen with a much slower decay time. Because of the microwave signal interference with the detector, this effect was almost overlooked as noise. With a 17 usec microwave pumping pulse, the laser oscillation was observed to last 300 usec. The estimated decay time constant is 100 usec.

To see if the observed long decay was really oscillation or a detector response transient, the helium and nitrogen supplies were shut off. Power dropped from 9.5 mw to 1.2 mw. The primary peak was between 1 and 2 usec duration and was comparable in height to the pulse obtained with all three gases. The laser pulse duration decreased to 10 usec with a time constant of 1-2 usec.

The photon lifetime in a cavity is defined as $(2 L/c)(1 - X)^{-1}$ [Ref 26:119] where X is the product of the resonator mirror reflectances. Assuming reflectances of 0.97 and 0.99, the photon lifetime is 0.3 usec. With gain present, the photon lifetime should be slightly longer than this.

The decay time constant for the laser output with pure CO_2 and the first pulse in the $CO_2:N_2:He$ are close to the photon lifetime. The delay in the initiation of the laser
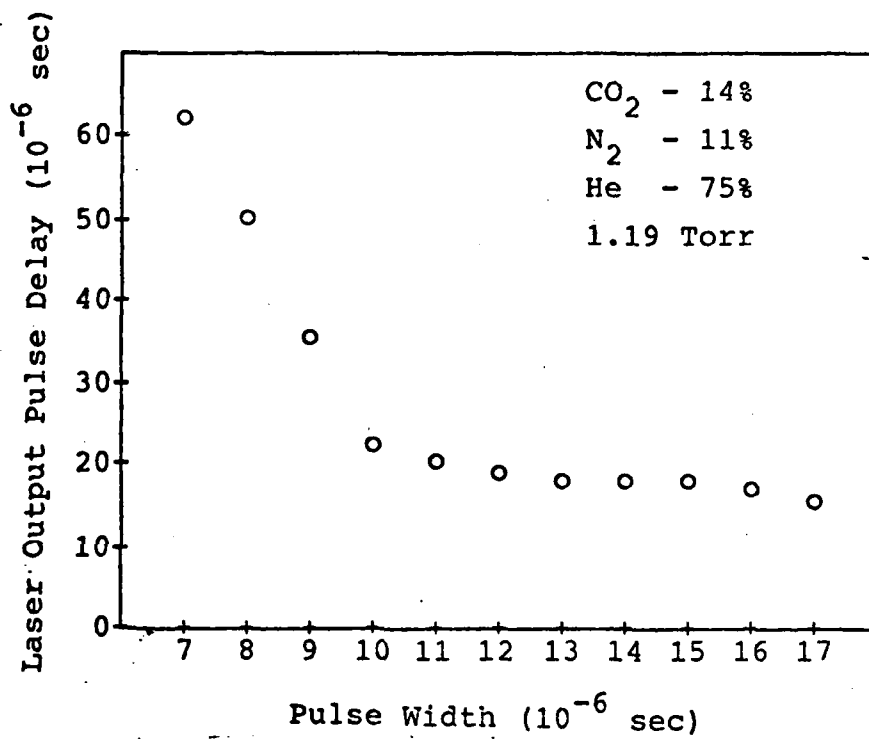
53

Figure 17. Laser delay from beginning of microwave pump pulse in a CO_2 laser as a function of input pulse width.
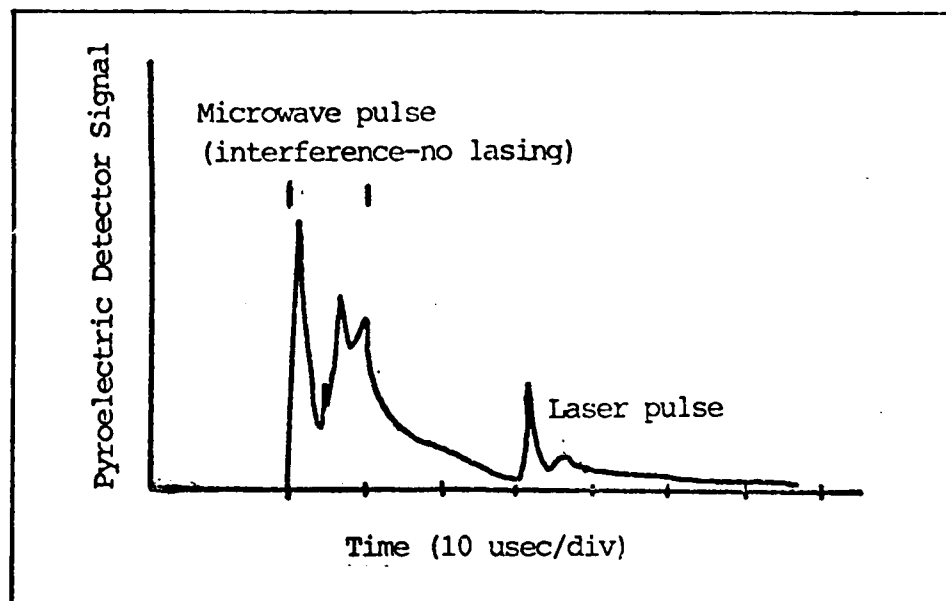
Figure 18. Pulse microwave pumped laser output.
The detector was a pyroelectric detector. Pulse
width 10 usec, 20 Hz repetition rate.

pulse, also observed by Handy and Brandelik, may be due to
dissociation of CO_2 [Ref 11:3755].

Looking at the resonant transfer of energy from the
excited N_2 to CO_2, the rate per volume of transfer of
energy quanta is the concentration of $CO_2/\tau vv$. Assuming
20% of the N_2 molecules are excited in the v=1 state (an
excitation temperature of $2000^{\circ}K$, a reasonable value),
$\tau_{vv}=5x10^{-3}$ sec. Assuming most of the CO_2 molecules are in
the ground state, the transfer rate is then $1.5x10^{19}$ sec^{-1}
in the active region and gas inlet arm of the tube. If all
the energy transferred goes into lasing, peak power due to
vibration-vibration transfer of energy is only 70 mw.

The resultant peak decay time for the $v=1$ N_2 is 1000 usec, ignoring all other loss mechanisms. While the estimated value differs by an order of magnitude from the calculated value, the resonant vibrational transfer of energy between N_2 and CO_2 is the probable cause of the observed effect.

Auxiliary Ionization With Pulsed Microwaves

The technique of using pulsed microwaves to provide the electron density and maintain the discharge was tried. This was examined for both CW microwave pumping and conventional DC pumping.

For CW microwave pumping, a threshold lasing level of 0.85 mw was established using one pulsed microwave source set with 8 usec pulse widths. CW microwave energy was then applied and power output increased steadily to 9.0 mw with an input CW microwave field of 180 watts. The gas mixture was 14:14:72 at 1.1 torr and a flow of 290 SCCM.

The experiment was repeated, decreasing the microwave pulses to a 4 usec duration and increasing the repetition rate to 1000 Hz. The gas mixture was optimized to 13:17:70 at 1.5 torr. In this setup, lasing did not occur from the pulsed microwave sustainer field. When the CW microwave field was brought to 45 watts, the laser generated 0.54 mw output. The output increased to 25 mw when the CW field was increased to 130 watts. At this point, a bright discharge formed at the gas inlet of the discharge tube. Power rapidly dropped to 3.5 mw.

Based on the work done by Hill [Ref 13], the pulsed sustainer field was increased to 18,000 Hz. Even though the microwave pulse was only 0.3 usec long, the laser output dropped for 20 usec with pure CO_2 as the lasing medium [Ref Fig 19].

By decreasing the repetition rate to 9600 Hz in a 17:8:75 gas mixture [Ref Fig 20], a quasi-CW output was obtained. The dip is still there, but less pronounced.

A possible cause of the dip is some of the CO_2 has been pumped to a high vibrational state which decays spontaneously to the (100), (020), (101) states, creating a bottleneck in the lower laser level. When the lower levels depopulate to the steady state energy distribution the laser output increases. The upper laser level does not seem to be affected because of the smooth (in the microsecond scale) decrease then increase in the laser output.

Another possible factor for the output dip is dissociation of CO_2 because the resulting oxygen relaxes the upper laser level. The low pressure involved would slow recombination processes just as the resonant energy transfer rate between N_2 and CO_2 is decreased.

The pulsed microwave sustainer was also tried in a number of configurations with DC pumping. Fig 21 shows the laser output and DC current passing through the discharge tube. The current displays an exponential decay. While the microwaves were necessary to maintain the discharge, significant ionization was present because of the DC field.
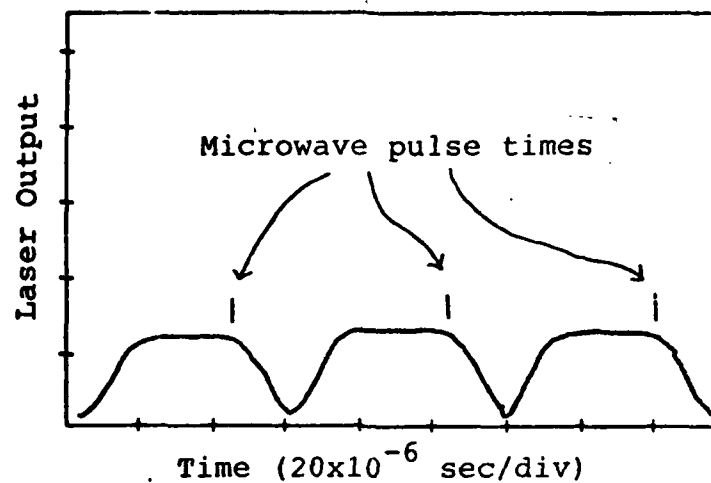
Figure 19. CO_2 laser pumped with a CW microwave field. The discharge is being maintained by an 18,000 Hz pulsed microwave field. The gas is 99% CO_2, with traces of He and N_2. Average power output is 9 mw.
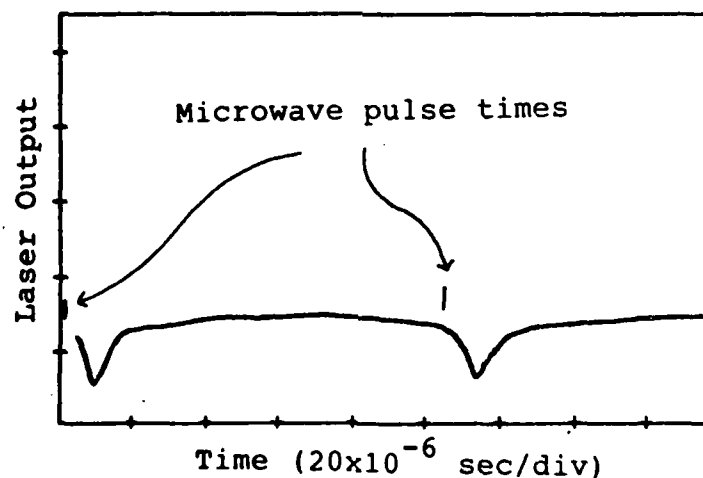

Figure 20. CO_2 laser pumped with a CW microwave field. The discharge is maintained by 9,600 Hz pulsed microwave field. The gas is 17% CO_2, 8% N_2, and 75% He. Average power output is 55 mw.
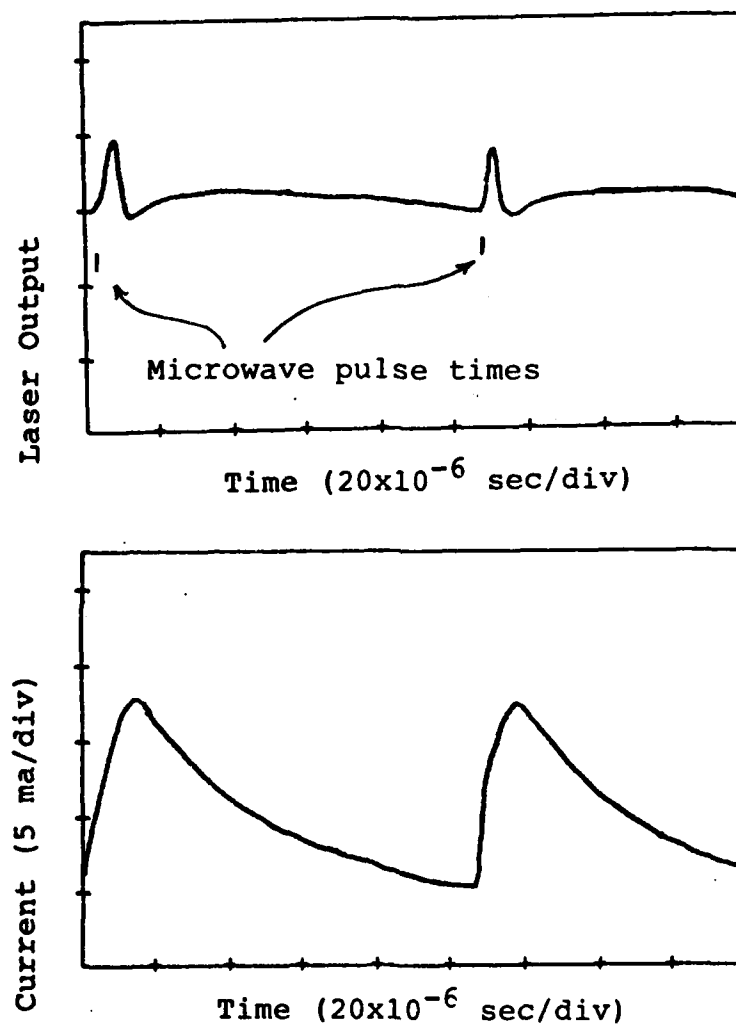
Figure 21. A DC current pumped laser with
the discharge sustained by a pulsed microwave
field. Gas mixture is 17% CO_2, 8% N_2,
and 74% He at 1 Torr. Average output is 55 mw.

59

Using an ambipolar diffusion coefficient of 1.1×10^4 cm^2/sec, the electron decay time is 2 usec.

Changing the pulsed microwave parameters and changing the gas mixture had profound impact on the appearance of the laser output. Fig 22 shows the result of having a discharge barely maintained by the DC potential. The microwave pulse width and power were adjusted until the sawtooth output was obtained. The discharge current averaged 5 ma.

Power output levels were typically around 60 mw using pulsed microwaves as an auxiliary source of ionization, a factor of two above the highest values obtained using DC pumping only.

While adjusting the microwave pulse width during the combined DC discharge and microwave avalanche ionization, the discharge would extinguish at specific pulse widths. This was looked at briefly. The underlying cause was capacitance of the cable combined with the high impedence of the ballast resistor. When the microwave initiates an ionization avalanche, current increases due to the increased electron density. The energy stored in the capacitance of the cable, approximately 420 picofarads, has enough energy to initiate an electron avalanche in the plasma. The high current of the avalanche drains the capacitor. The R-C time constant is 84 usec. If the supply voltage is below the sparking potential of the gas and the electron density decays enough, the discharge will
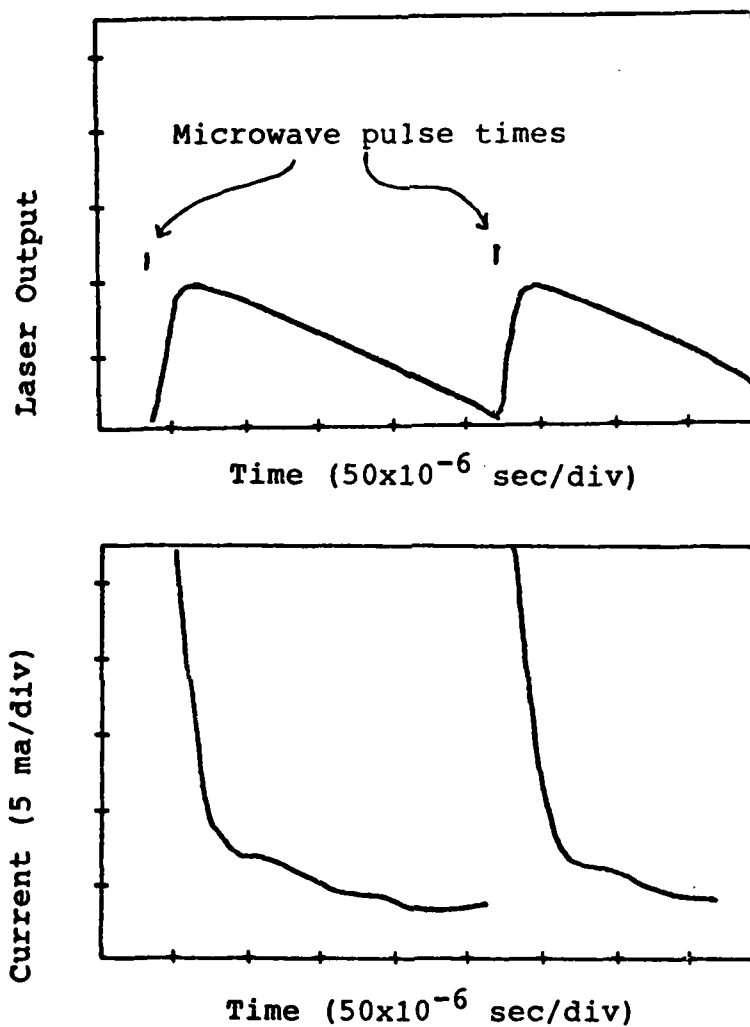
Figure 22. Sawtooth modulation from a DC current
pumped laser with the discharge assisted by a
pulsed microwave field. Gas mixture is 46% CO_2,
27% N_2, and 27% He at 0.5 Torr. Average output
is 70 mw.

extinguish. Fig 23 shows the tube current and voltage measured from the ballast resistor for a $CO_2:N_2$ mixture. A discharge in a mixture of 95% CO_2 and 5% N_2 would extinguish on the average on every third pulse with pulses spaced about 2 seconds apart. The original current was 4 ma and the tube potential was 3.5 kV.
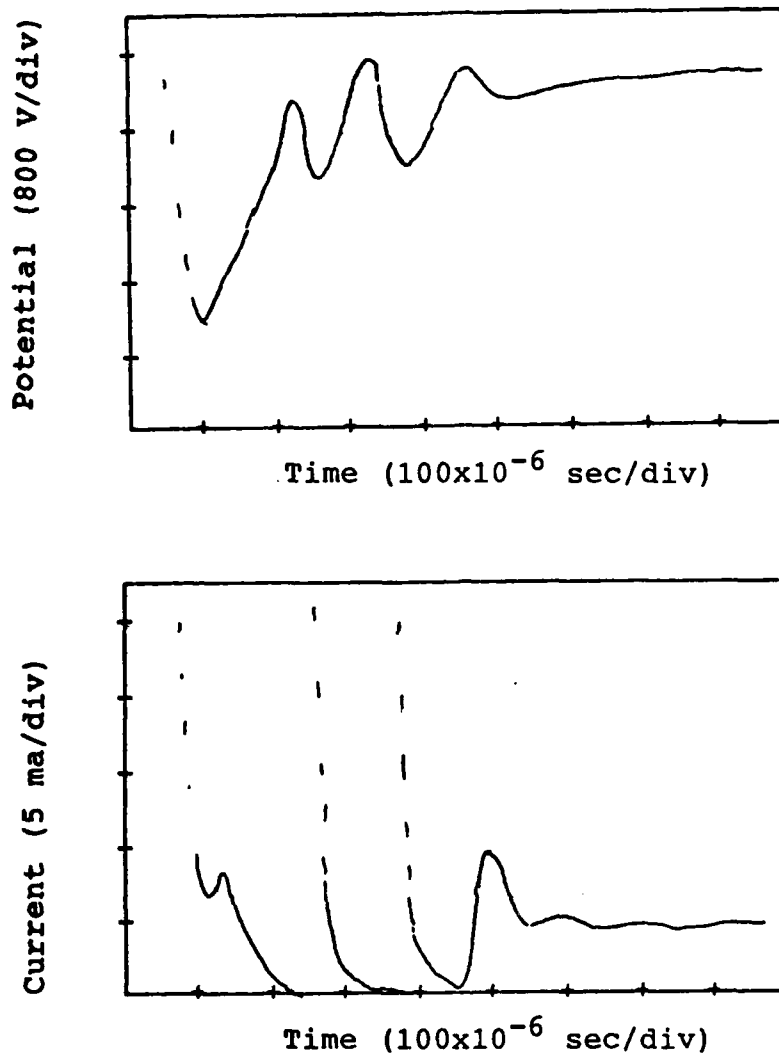
Figure 23. DC discharge quenching due to
avalanche ionization from pulsed microwaves. The
gas mixture here is 11% CO_2 and 89% N_2 at 0.2
torr. The time constant associated with the
resistance of the ballast resistor and the
capacitance of the connecting cable can cause a
discharge to extinguish when an avalanche is
initiated by microwaves. The gas mixture was
adjusted so ringing could be observed from the
initial avalanche.

63

VI. Conclusions and Recommendations

Many questions remain unanswered concerning the use of microwaves for pumping of lasers. There is no problem getting microwave energy coupled into the laser mixes. It is probably more of a problem to decouple the plasma more from the microwave field. Because most of the microwaves were absorbed by the plasma, each region of the discharge was competing for the available energy which contributed to the local nature of the CW microwave discharges.

Microwave Discharges

CW microwave discharges were localized at incident power levels of interest for lasing. To get a near-uniform discharge, input power levels had to be around 200 watts. This undoubtedly caused tremendous heating of the plasma. Gain measurement was attempted in a $CO_2:N_2:He$ laser mix. If any gain was present, it was too small to detect with the equipment in use.

The pulsed microwave discharges appeared uniform throughout the plasma tube in the applicator region. This is consistent with the observation of CW discharges tending to become more uniform as microwave power was increased.

Microwave Excitation

The pulsed microwaves alone were able to pump a standard $CO_2:N_2:He$ laser mix and make it lase. Power

64

output was low, due in part to the narrow bore plasma tube in use. Typical power out was 5 mw average when pulsed at 200 Hz. The laser pulses consisted of one narrow 'intense' of about 2 usec duration and a less intense one which had a decay rate estimated to be around 100 usec. Based on an effective pulse width of 2 usec, the intense pulse has a peak power of 2 watts.

The delay times for laser initiation were from 17 usec to over 100 usec from the firing of the microwave pulse. As the pulse widths were increased, the delays approached the 17 usec time in what appeared to be asymptotically.

Avalanche Ionization

By a controlled avalanche ionization, it is possible to lower the E/n ratio in a discharge to get more efficient pumping. While lasing was never obtained pumping with CW microwaves only, pulsed microwaves were successfully used to maintain a uniform discharge which allowed pumping from the CW microwaves. A maximum of 70 mw average laser power was obtained using this technique. However, the CW microwave field did cause localized discharges to form when the microwave field became too intense.

The pulsed microwaves were also used to enhance the output of the laser when pumping was being accomplished by DC current. The output when pumping was done by DC was typically 25 mw. A combination of DC pumping with an avalanche ionization increased the power to 50 mw.

Recommendations

While the results seem to look favorable compared to the DC benchmark for various laser pumping schemes using microwaves, it should be remembered the low efficiencies obtained by all the methods. None of the results gave obvious indications of what the scalability is of microwave excitation methods.

Some useful information would be what is happening in the microwave discharge. This may help to decouple the plasma from the microwave field slightly and improve uniformity of the discharge.

The present equipment could be used for further experimentation of microwave excitation. While the applicators were separated by at least 3 cm for the experiments here, it is possible they should be placed closer together. If further work is to be done with the CO_2 laser, the use of a larger diameter tube and/or higher pressure is recommended so the pD product for CO_2 is closer to the optimum value of 2 torr-cm. Of possible benefit would be another pulsed microwave source with more power available to assist in getting discharges in higher pressure media. That step may mean using a different applicator.

Bibliography

1. Allis, W. P.; S. C. Brown; and E. Everhart. "Electron density distribution in a high frequency discharge in the presence of plasma resonance," The Physical Review, 84:519-522 (1951).

2. Bekefi, G. Radiation Processes in Plasmas. New York: John Wiley and Sons, Inc., 1966.

3. Bollen, W. M.; C. P. Christensen; R. W. Waynant; and R. L. Burnham. Microwave Conditioned DC Discharges for Excitation of Rare-Gas-Halide Lasers. Report for Naval Research Laboratory, contract N00014-82-C-2257. Alexandria: Mission Research Corporation, December 1982.

4. Chen, F. F. Introduction to Plasma Physics. New York: Plenum Press, 1977.

5. Cheo, P. K. "CO_2 Lasers," Lasers, edited by Levine and DeMaria. New York: Marcel Dekker, Inc., 1971.

6. Darrah, R. and M. L. Andrews. Microwave Plasma Excitation. Quarterly progress report #1 under contract F-33615-75-C-1082, Task 2 (Universal Energy Systems, Inc.) and contract F-33615-73-C-4155, Task 9 (Technology, Inc) under sponsorship of Aero Propulsion Laboratory, Wright Patterson Air Force Base, Ohio, June 1975.

7. Demaria, A. J. "Review of CW High-Power CO Lasers," Proceedings of the IEEE, 61 (6):731-748 (June 1973).

8. Douglas-Hamilton, D. H. and R. S. Lowder. Carbon Dioxide Electric Discharge Laser Kinetics Handbook. Final report AFWL-TR-74-216, (1974).

9. Duley, W. W. CO_2 Lasers, Effects and Applications. New York: Academic Press, 1976

10. Everhart, E. and S. C. Brown. "The Admittance of High Frequency Gas Discharges," Physical Review, 76 (6):839-842 (15 September 1949).

11. Handy, K. G. and J. E. Brandelik. "Laser generation by pulsed 2.45 GHz microwave excitation of CO_2," Journal of Applied Physics, 49 (7):3753-3756 (July 1978).

12. Heald, M. A. and C. B. Wharton. *Plasma Diagnostics With Microwaves*. New York: John Wiley & Sons, Inc., 1965.

13. Hill, A. E. "Continuous uniform excitation of medium-pressure CO laser plasmas by means of controlled avalanche ionization," *Applied Physics Letters*, 22 (12):670-673 (15 June 1973).

14. Holt, E. H. and R. E. Haskell. *Foundations of Plasma Dynamics*. New York: The Macmillan Company, 1965.

15. Lachambre, J.; J. Macfarlane; G. Otis; and P. Lavigne. "A transversely rf-excited CO_2 waveguide laser," *Applied Physics Letters*, 32 (10):652-653 (15 May 1978).

16. Llewellyn-Jones, F. *The Glow Discharge*. London: Methuen & Co. LTD, 1966.

17. Lotkova, E. N.; V. N. Ochkin; and N. N. Sobolev. "Dissociation of Carbon Dioxide and Inversion in CO_2 Laser," *IEEE Journal of Quantum Electronics*, 7 (8):396-402 (August 1971).

18. Lovold, S. *Continuously-Tunable High-Repetition Rate RF-Excited CO_2 Waveguide Laser*. Kjeller, Norway: Norwegian Defence Research Establishment, (NDRE/PUBL-82/1002), 12 July 1982.

19. Lovold, S. and G. Wang. *Ten Atmospheres High Repetition Rate RF-Excited CO_2 Laser*. Kjeller, Norway: Norwegian Defence Research Establishment, 1981 (unknown if formally published).

20. MacDonald, A. D. *Microwave Breakdown in Gases*. New York: John Wiley & Sons, Inc., 1966.

21. Rensch, D. B. *A Parameter Study of a Carbon Dioxide Gas Laser*. Prepared for NASA, Grant Number NSG-74-60. Columbus, Ohio: The Ohio State University Research Foundation, 15 November 1966.

22. Svelto, O. *Principles of Lasers*, (Second Edition). New York: Plenum Press, (1982).

23. Thorne, J. *Discharge Under the Combined Influence of DC and RF Fields*, MS thesis. Wright-Patterson AFB, Ohio: Air Force Institute of Technology, December 1982.

24. Tychinskii, V. P. "Powerful Gas Lasers," _Soviet Physics Uspeckhi_, _10_ (2):131-151 (September-October 1967).

25. Vasyutinskii, O. S., _et al_. "Pulsed microwave discharge as a pump for the CO_2 laser," _Soviet Physics, Technical Physics_, _23_ (2):189-194 (February 1978).

26. Verdeyen, Joseph T. _Laser Electronics_. Englewood Cliffs, New Jersey: Prentice Hall, Inc., 1981.

Appendix A. ABCD Matrix Solution of a Stable Cavity

This section is devoted to developing eqs (17, 18, 19), for determing spot sizes, waist size and location. The technique used is matrix ray tracing. Throughout the development, references will be made primarily to [26] which contains all the information needed concerning the use of the complex beam parameter q.

The parameters for the cavity in Figure A-1 will be used to set up the ray matrix. The first step is to find the values for the ABCD matrix, based on a round trip path through the cavity.
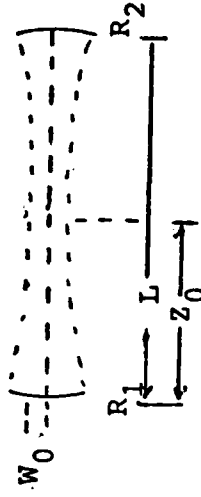

Figure A-1. Cavity parameters

$$\begin{bmatrix} A & B \\ C & D \end{bmatrix} = \begin{bmatrix} 1 & 0 \\ -2/R_1 & 1 \end{bmatrix}\begin{bmatrix} 1 & L \\ 0 & 1 \end{bmatrix}\begin{bmatrix} 1 & 0 \\ -2/R_2 & 1 \end{bmatrix}\begin{bmatrix} 1 & L \\ 0 & 1 \end{bmatrix} \tag{A-1}$$

$$\begin{bmatrix} A & B \\ C & D \end{bmatrix} = \begin{bmatrix} 1 & L \\ -2/R_1 & (-2L/R_1 + 1) \end{bmatrix}\begin{bmatrix} 1 & L \\ -2/R_2 & (-2L/R_2 + 1) \end{bmatrix} \tag{A-2}$$

$$\begin{bmatrix} A & B \\ C & D \end{bmatrix} = \begin{bmatrix} (1 - 2L/R_2) & (L - 2L^2/R_2 + L) \\ (-2/R_1 + 4L/R_1R_2 - 2/R_2) & (-4L/R_1 + 4L^2/R_1R_2 - 2L/R_2 + 1) \end{bmatrix} \tag{A-3}$$

A-1

If this is to be a stable cavity, beam parameters must not change on the round trip. For Gaussian beams

$$q_2 = \frac{Aq_1 + B}{Cq_1 + D} \qquad (A-4)$$

[Ref 26:73]

where q is the complex beam parameter. In a stable cavity, $q_1 = q_2$, so

$$q_1 = \frac{Aq_1 + B}{Cq_1 + D} \qquad (A-5)$$

By rearranging terms

$$Cq_1^2 + q_1(D - A) - B = 0 \qquad (A-6)$$

which can be solved by the quadratic equation to yield

$$q_1 = \frac{A - D}{2C} \pm \frac{1}{2C}(D^2 - 2AD + A^2 + 4BC)^{1/2} \qquad (A-7)$$

Whenever the index of refraction at the exit plane of the transfer matrix is the same as at the entrance plane, the determinant is equal to one [Ref 25:27], so

A-2

AD − BC = 1 (A-8)

Solving this for BC and substituting into eq (A-7) we get

$$q_1 = \frac{A-D}{2C} \pm \frac{1}{2C}(D^2 + 2AD + A^2 - 4)^{1/2}$$ (A-9)

Immediately this simplifies to

$$q_1 = \frac{A-D}{2C} \pm \frac{1}{2C}[(D + A)^2 - 4]^{1/2}$$ (A-10)

For the parameter q_1 to be complex, $[(D + A)^2 - 4] < 0$ immediately yields

$$\frac{(D + A)^2}{4} < 1$$ (A-11)

This establishes the stability condition which must be met for a stable cavity to exist

$$\left| \frac{A + D}{2} \right| < 1 \qquad \text{(Stability Condition)}$$ (A-12)

Substituting the matrix elements from eq (A-3)

A-3

which simplifies to

$$\frac{A+D}{2} = \left(2 - \frac{4L}{R_1} - \frac{4L}{R_2} + \frac{4L^2}{R_1 R_2}\right)\frac{1}{2} \qquad \text{(A-13)}$$

$$\frac{A+D}{2} = 2\left(1 - \frac{L}{R_1}\right)\left(1 - \frac{L}{R_2}\right) - 1 \qquad \text{(A-14)}$$

Applying the stability condition from eq (A-12) to eq (A-14) yields

$$0 < \left(1 - \frac{L}{R_1}\right)\left(1 - \frac{L}{R_2}\right) < 1 \qquad \text{(A-15)}$$

which is the final criterion for the stability of a cavity, based solely on the geometric considerations.

The next consideration is the complex parameter q to extract information of the beam size at various locations in the cavity. The complex parameter is related to the beam characteristics by

$$\frac{1}{q} = \frac{1}{R} - j\frac{Y}{\pi W^2} \qquad \text{(A-16)}$$

[Ref 26:74]

A-4

where Y is the wavelength of the light in the cavity, R is the radius of curvature of the wavefront, and W is the beam radius. Dividing eq (A-6) by $-(1/q_2)^2$

$$-C - \frac{D-A}{q_1} + B \frac{1}{q_1^2} = 0 \qquad (A-17)$$

Applying the quadratic formula and eq (A-8),

$$\frac{1}{q_1} = \frac{A-D}{2B} \overset{+}{\underset{-}{}} \frac{1}{2B}((D+A)^2 - 4)^{1/2} \qquad (A-18)$$

By removing $j=(-1)^{1/2}$ from the square root term, of eq (A-18) and combining with eq (A-16) we get

$$\frac{1}{q_1} = \frac{D-A}{2B} \overset{+}{\underset{-}{}} j\frac{1}{2B}(4 - (D+A)^2)^{1/2} = \frac{1}{R} - j\frac{Y}{\pi W^2} \qquad (A-19)$$

The complex beam parameter varies simply with the displacement z such that $q = q_1 + z$. From this we can now find the location and radius of the waist of the cavity. Intuitively the radius of curvature of the beam will be infinite at the beam waist. The beam parameter at the waist is then

$$q_0 = q_1 + z_0 = -j \; \frac{\pi w_0^2}{\gamma} \qquad \text{(A-20)}$$

Taking this and eq (A-10) leads immediately to

$$z_0 = -Re(q_1) = -\frac{A - D}{2C} \qquad \text{(A-21)}$$

Substituting the matrix elements

$$z_0 = \frac{1 - 2L/R_2 + 4L/R_1 + 2L/R_2 - 4L^2/R_1R_2 - 1}{-2(-2/R_1 + 4L/R_1R_2 - 2/R_2)} \qquad \text{(A-22)}$$

The following steps are simplifications of eq (A-22)

$$z_0 = \frac{4(L/R_1)(1 - L/R_2)}{(-2/L)(-2L/R_1 + 4L^2/R_1R_2 - 2L/R_2)} \qquad \text{(A-23)}$$

$$z_0 = \frac{L4(L/R_1)(1-L/R_2)}{4(L/R_1 + L/R_2 - 2L^2/R_1R_2)} \qquad \text{(A-24)}$$

$$z_0 = \frac{L(L/R_1)(1 - L/R_2)}{(-1 + L/R_1 - 1 + L/R_2 + 2 - 2L^2/R_1R_2)} \qquad \text{(A-25)}$$

$$z_0 = \frac{L(L/R_1)(1 - L/R_2)}{(-1 + L/R_1 - 1 + L/R_2 - 2(-1 + L^2/R_1R_2))}$$ (A-26)

$$z_0 = \frac{L(L/R_1)(1-L/R_2)}{-1 + L/R_1 -1 + L/R_2 - 2(-1 -L/R_1 - L/R_2 + L^2/R_1R_2 + L/R_1 + L/R_2)}$$ (A-27)

$$z_0 = \frac{L(L/R_1)(1 - L/R_2)}{-1 + L/R_1 -1 + L/R_2 - 2((1-L/R_1)(1-L/R_2) -1 + L/R_1 -1 + L/R_2)}$$ (A-28)

$$z_0 = \frac{L(L/R_1)(1 - L/R_2)}{1 - L/R_1 + 1 - L/R_2 - 2(1-L/R_1)(1-L/R_2)}$$ (A-29)

Now defining the dimensionless quantities

$$G_1 = (1 - L/R_1)$$ (A-30)

$$G_2 = (1 - L/R_2)$$ (A-31)

eq (A-29) becomes

$$z_0 = \frac{L(1-G_1)(G_2)}{(G_1 + G_2 - 2G_1G_2)}$$ (A-32)

A-7

which gives the location of the beam waist measured from mirror #1. Now we must examine the size of the waist, which will be useful in determing the spot size at various locations in the cavity. From eq (A-20)

$$Im(q_0) = Im(q_1) = -\frac{\pi W_0^2}{Y}$$

(A-33)

Removing $(-1)^{1/2}$ from eq (A-10) and combining with eq (A-33)

$$W_0^2 = -\frac{Y}{\pi}\frac{1}{2C}(4 - (D + A)^2)^{1/2}$$

(A-34)

Substituting the matrix elements

$$W_0^2 = -\frac{Y L(4 - (2 - 4L/R_2 - 4L/R_1 + 4L^2/R_1R_2)^2)^{1/2}}{\pi -4(G_1 + G_2 - 2G_1G_2)}$$

(A-35)

Recalling that $a^2 - b^2 = (a + b)(a - b)$,

$$W_0^2 = \frac{Y L((2 + 2 - 4L/R_2 -4L/R_1 + 4L2/R_1R_2)(4L/R_2 + 4L/R_1 - RL^2/R_1R_2))^{1/2}}{\pi 4(G_1 + G_2 - 2G_1G_2)}$$

(A-36)

A-8

$$W_0^2 = \frac{Y \, L \, (4(G_1 G_2)(4)(1 - 1 + L/R_2 + L/R_1 - L^2/R_1 R_2))^{1/2}}{\pi \, 4(G_1 + G_2 - 2G_1 G_2)} \qquad \text{(A-37)}$$

This finally reduces to

$$W_0 = \frac{Y \, L \, ((G_1 G_2)(1-G_1 G_2))^{1/2} \, ^{1/2}}{\pi \, (G_1 + G_2 - 2G_1 G_2)} \qquad \text{(A-38)}$$

Now for any stable cavity, we have analytical values for W_0 and z_0. The spot size for any location in the cavity can be calculated from

$$q(z) = q_0 + z' \qquad \text{(A-39)}$$

and

$$\frac{1}{q(z)} = \frac{1}{R} - j \, \frac{Y}{\pi W^2} \qquad \text{(A-16)}$$

where $z' = 0$ at $z = z_0$. Now we define

$$Q_0 = \frac{\pi W_0^2}{Y} \qquad \text{(A-40)}$$

so that eq (A-20) can now be expressed as

$$\frac{1}{q(z)} = \frac{1}{jQ_0 + (z - z_0)} \tag{A-41}$$

$$\frac{1}{q(z)} = \frac{(z - z_0) - jQ_0}{(z - z_0)^2 + Q_0^2} \tag{A-42}$$

From eqs (A-42) and (A-16) we now get

$$W = ((Y/\pi)\,((z - z_0)^2 + Q_0^2)/Q_0)^{1/2} \tag{A-43}$$

This completes the development of the equations for stable cavity calculations. The steps to follow for analyzing the stability of a cavity and resulting beams sizes are now quite simple. First, determine if the cavity is stable using the stability condition summarized in eq (A-15). If the cavity is stable, the beam waist location can be found from eq (A-32) and the beam size at the waist found from eq (A-38). The beam size at any location in the cavity is given by eq (A-43). Appendix B contains a listing of a BASIC program which can be used to perform these calculations on most home computer systems.

Appendix B.   Resonator Design Program

```
10 REM — Resonator Design Program for Microsoft BASIC
11 REM    Richard C. Page, Capt, USAF, June 1983
12 REM    ---------------------------------------------
13 REM    This simple program will determine if a resonator
14 REM    cavity is stable (has a Gaussian solution).  If
15 REM    the cavity is stable, the waist size and location
16 REM    are given in addition to the spot sizes at each
17 REM    of the mirrors.  Spot sizes can also be computed
18 REM    for any location in the cavity.
19 '---------------------------------------------
20 'D   - Resonator length (meters)
21 'G1  - Dimensionless cavity parameter
22 'G2  - Dimensionless cavity parameter
23 'GG  - G1*G2
24 'PI  - 3.14159
25 'R1  - Radius of curvature of mirror #1 (meters)
26 'R2  - Radius of curvature of mirror #2 (meters)
27 'W   - Spot size at location Z (meters)
28 'W0  - Waist Size (meters)
29 'W1  - Spot size at mirror #1 (meters)
30 'W2  - Spot size at mirror #2 (meters)
31 'Y   - Wavelength (meters)
32 'YY  - Wavelength (microns)
33 'Z   - Location in cavity (meters)
34 'Z1  - Location of waist (meters)
35 '---------------------------------------------
90    PI=ATN(1)*4
100   PRINTR1,:INPUT"Radius of curvature of mirror #1 (meters)";R1
110   PRINTR2,:INPUT"Radius of curvature of mirror #2 (meters)";R2
120   PRINTD,:INPUT"Distance between mirrors (meters)";D
130   PRINTYY,:INPUT"Wavelength (microns)";YY
140   Y=YY*1E-6: REM  convert to meters
150   G1=1-(D/R1)
160   G2=1-(D/R2)
170   GG=G1*G2
180   IF (GG<=0) OR (GG>1) THEN GOTO 200
190   GOTO 220
200   PRINT"Unstable Configuration - G1*G2 =";GG
210   GOTO 100
220   W1= SQR( (Y/PI) * D*G2 / SQR(G1*G2*(1-G1*G2)))
230   W2= SQR( (Y/PI) * D*G1 / SQR(G1*G2*(1-G1*G2)))
240   Z1=D*G2*(1-G1)/(G1+G2-2*G1*G2)
250   W0=SQR( (Y/PI)* (D/(G1+G2-2*G1*G2)) * SQR(G1*G2*(1-G1*G2)))
260   PRINT"Waist =";W0;"meters    at ";Z1" meters from mirror #1
270   PRINT"Spot Sizes — Mirror #1=";W1;"  Mirror #2=";W2;" (meters)
280   Q0 = W0↑2*PI/Y
290   Z=0:INPUT"Find Spot Size for Location (meters)";Z
300   IF Z=0 GOTO 100
310   W=SQR( (Y/PI) * ( (Z1-Z)↑2 +Q0↑2)/Q0)
320   PRINT "Loc =";Z;" (meters)  Radius =";W;" (meters)"
330   GOTO 290
```

Sample Output:


```
READY
>RUN
  0              Radius of curvature of mirror #1 (meters)? 2.5
  0              Radius of curvature of mirror #2 (meters)? 2.5
  0              Distance between mirrors (meters)? 1.04
  0              Wavelength (microns)? 10.6
Waist = 1.85031E-03 meters     at  .52  meters from mirror #1
Spot Sizes -- Mirror #1= 2.07913E-03   Mirror #2= 2.07913E-03   (meters)
Find Spot Size for Location (meters)? .1
Loc = .1  (meters)  Radius = 2.00255E-03   (meters)
Find Spot Size for Location (meters)? .2
Loc = .2  (meters)  Radius = 1.94014E-03   (meters)
Find Spot Size for Location (meters)? 0
  2.5            Radius of curvature of mirror #1 (meters)? 1E38
  2.5            Radius of curvature of mirror #2 (meters)? 2.5
  1.04           Distance between mirrors (meters)?
  10.6           Wavelength (microns)?
Waist = 2.03903E-03 meters     at  0  meters from mirror #1
Spot Sizes -- Mirror #1= 2.03903E-03   Mirror #2= 2.6682E-03   (meters)
Find Spot Size for Location (meters)? .1
Loc = .1  (meters)  Radius = 2.04574E-03   (meters)
Find Spot Size for Location (meters)? .5
Loc = .5  (meters)  Radius = 2.2005E-03   (meters)
Find Spot Size for Location (meters)? .9
Loc = .9  (meters)  Radius = 2.525E-03   (meters)
Find Spot Size for Location (meters)? 0
  1E+38          Radius of curvature of mirror #1 (meters)?
Break in 100
READY
>
```

Richard Charles Page was born in Dodgeville, Wisconsin on 24 April 1948. After graduating in 1967 from high school in Rochelle, Illinois, he enlisted in the United States Air Force and served four years as a pest control operator. After his tour of duty, he returned to Rochelle where he was employed as a newspaper photographer. He later attended Northern Illinois University and received a Bachelor of Science degree in physics in June 1977. He received a commission in the United States Air Force through Officer Training School. He was assigned as a systems analyst to Air Force Wright Aeronautical Laboratories, Avionics Laboratory, until his entry into the School of Engineering, Air Force Institute of Technology in June 1982.

Permanent address: 950 N 14th Street

Rochelle, Illinois 61068

END
FILMED
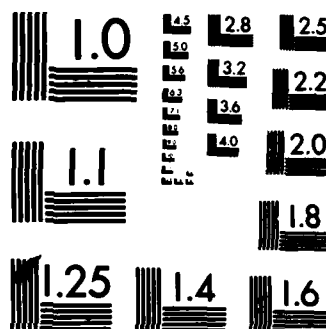
MICROCOPY RESOLUTION TEST CHART
NATIONAL BUREAU OF STANDARDS-1963-A

REPORT DOCUMENTATION PAGE

1a. REPORT SECURITY CLASSIFICATION UNCLASSIFIED	1b. RESTRICTIVE MARKINGS
2a. SECURITY CLASSIFICATION AUTHORITY	3. DISTRIBUTION/AVAILABILITY OF REPORT
2b. DECLASSIFICATION/DOWNGRADING SCHEDULE	Approved for public release; distribution unlimited

4. PERFORMING ORGANIZATION REPORT NUMBER(S)	5. MONITORING ORGANIZATION REPORT NUMBER(S)
AFIT/GEP/PH/83D-8	

6a. NAME OF PERFORMING ORGANIZATION	6b. OFFICE SYMBOL (If applicable)	7a. NAME OF MONITORING ORGANIZATION
School of Engineering	AFIT/EN	

6c. ADDRESS (City, State and ZIP Code)	7b. ADDRESS (City, State and ZIP Code)
Air Force Institute of Technology Wright-Patterson AFB, OHIO 45433	

8a. NAME OF FUNDING/SPONSORING ORGANIZATION	8b. OFFICE SYMBOL (If applicable)	9. PROCUREMENT INSTRUMENT IDENTIFICATION NUMBER
Energy Conversion Branch	AFWAL/POOC-3	

8c. ADDRESS (City, State and ZIP Code)	10. SOURCE OF FUNDING NOS.			
	PROGRAM ELEMENT NO.	PROJECT NO.	TASK NO.	WORK UNIT NO.
11. TITLE (Include Security Classification) See Block 19				

12. PERSONAL AUTHOR(S)
Richard C. Page, BS, Capt, USAF

13a. TYPE OF REPORT	13b. TIME COVERED	14. DATE OF REPORT (Yr., Mo., Day)	15. PAGE COUNT
MS Thesis	FROM _____ TO _____	December 1983	95

16. SUPPLEMENTARY NOTATION

LYNN E. WOLAVER 7 Feb 84
Dean for Research and Professional Development
Air Force Institute of Technology (ATC)
Wright-Patterson AFB OH 45433

17. COSATI CODES			18. SUBJECT TERMS (Continue on reverse if necessary and identify by block number)
FIELD	GROUP	SUB. GR.	Lasers; Laser Pumping; Carbon Dioxide Lasers; Infrared Lasers; Microwaves; Excitation
20	05		

19. ABSTRACT (Continue on reverse if necessary and identify by block number)

Thesis Title: Microwave Excitation of a CO_2 Laser

Thesis Chairman : William F. Bailey, PhD, Lt Col, USAF

20. DISTRIBUTION/AVAILABILITY OF ABSTRACT	21. ABSTRACT SECURITY CLASSIFICATION
UNCLASSIFIED/UNLIMITED ☒ SAME AS RPT. ☐ DTIC USERS ☐	UNCLASSIFIED

22a. NAME OF RESPONSIBLE INDIVIDUAL	22b. TELEPHONE NUMBER (Include Area Code)	22c. OFFICE SYMBOL
William F. Bailey , PhD, Lt Col, USAF	513/255-2012	AFIT/ENP

A flowing carbon dioxide laser was operated at low pressures up to 4 torr. Excitation of the laser was provided using various combinations of direct current (DC), pulsed microwave, and continuous wave (CW) microwave excitation. The microwaves were in the 2.45 GHz band and were coupled into the gas using a slow-wave interdigital transmission line. Laser output of 25 milliwatts (mw) was achieved using a DC discharge only. A combination of a DC discharge and pulsed microwaves doubled the output and resulted in some modulation. Changing the laser gas mixture and pulsed microwave field characteristics allowed some flexibility in the modulation. Lasing was not achieved with excitation from the CW microwaves alone due to the formation of localized discharges. Using pulsed microwaves to sustain the discharge and CW microwaves to pump the laser, a quasi-CW output of 55 mw was achieved.